LIBRARY
FISH & WILDLIFE SERVICE
PACIFIC OCEANIC FISHERY
INVESTIGATIONS

SEARS FOUNDATION FOR MARINE RESEARCH
BINGHAM OCEANOGRAPHIC LABORATORY, YALE UNIVERSITY

JOURNAL OF MARINE RESEARCH

VOLUME VI, 1947

NUMBER 2

ISSUED JUNE 30, 1947, NEW HAVEN, CONN., U. S. A.

JOURNAL OF MARINE RESEARCH

PUBLISHED BY

SEARS FOUNDATION FOR MARINE RESEARCH
BINGHAM OCEANOGRAPHIC LABORATORY, YALE UNIVERSITY

BOARD OF EDITORS

Chairman: A. E. PARR
American Museum of Natural History, New York

C. O'D. ISELIN
Woods Hole Oceanographic Institution

H. U. SVERDRUP
Scripps Institution of Oceanography

DANIEL MERRIMAN
Bingham Oceanographic Laboratory

C.-G. ROSSBY
University of Chicago

THOMAS G. THOMPSON
Oceanographic Laboratories, University of Washington

MANAGING EDITOR

YNGVE H. OLSEN
Bingham Oceanographic Laboratory
Yale University
New Haven, Conn.

The Journal is normally issued in three numbers per year constituting one volume, except for 1942 through 1945, when only one volume was published. Volume VI will be completed in 1947. All the income derived from subscriptions will be used solely to increase the volume and improve the quality of the Journal for the benefit of its subscribers and contributors.

Subscription price three dollars per volume, or one dollar per number. Address all communications to the Managing Editor. See inside rear cover for Note to Authors.

SEARS FOUNDATION FOR MARINE RESEARCH
BINGHAM OCEANOGRAPHIC LABORATORY, YALE UNIVERSITY

JOURNAL OF
MARINE RESEARCH

VOLUME VI 1947 NUMBER 2

NOTE ON THE USE OF THE *T-S* CORRELATION FOR DYNAMIC HEIGHT ANOMALY COMPUTATIONS[1]

By

HENRY STOMMEL
Woods Hole Oceanographic Institution

1. The convenience of the bathythermograph for making rapid detailed surveys of the thermal structure in vertical sections of the ocean is leading to an accumulation of data on ocean temperatures far exceeding that on the corresponding salinities. Since dynamic height anomaly computations require a knowledge of both the temperature and the salinity as functions of depth, it is the purpose of this note to determine, in the case where only temperature data are available, whether or not it is possible to use the known *T-S* correlation for a given water mass to supply information on salinity which is sufficiently accurate to be used in dynamic height and current computations.

2. The functional relation between T and S, as shown by the *T-S* diagram for any particular water mass, is such that for a given temperature T the value of salinity S is given only within a certain "range of uncertainty," which is denoted by R_s. The quantity R_s varies for different water masses and also for different temperatures within the same water mass.

From a knowledge of the approximate dependence of R_s upon the pressure (depth) a rough estimate of the range of uncertainty R_D in the dynamic height may be made. For these purposes the *T-S* curve is divided into pressure intervals Δp of approximately constant R_s.

[1] Contribution No. 367 from the Woods Hole Oceanographic Institution.

Calculation of the mean range of uncertainty in the specific volume anomaly (indicated by R_δ) is then possible for each Δp. The products $R_\delta \cdot \Delta p$ are formed and summed up from the surface to the depth of the pressure reference level. The final quantity $\Sigma R_\delta \cdot \Delta p$ may be written as R_D. Because this represents the entire range of uncertainty in the determination of the dynamic height, the probable error in dynamic height may be taken as about $\pm \frac{1}{4} R_D$.

To facilitate this operation—which need merely be approximate—Table I has been constructed. It is prepared directly from the usual tables for δ_s (1, 4).

TABLE I—Brief Table for Approximate Calculation of the Uncertainty in Specific Volume Anomaly from the Uncertainty in Salinity

Salinity Uncertainty	*Specific Volume Anomaly Uncertainty*	*Salinity Uncertainty*	*Specific Volume Anomaly Uncertainty*
R_s(°/oo)	R_δ	R_s(°/oo)	R_δ
0.00	0.00000	0.30	0.00023
.02	2	.40	30
.04	3	.50	38
.06	5	.60	46
.08	6	.70	53
.10	8	.80	61
.15	11	.90	69
.20	15	1.00	76
.25	19	2.00	152

As an example of the use of Table I, some stations made at the Grand Banks in June 1940 by the International Ice Patrol (3) are considered. Rather than include a great number of stations the discussion will be limited to the small area covered by stations 3275, 3276, 3277, and 3278. Upon plotting these data on a *T-S* plane it is immediately apparent that the curve may be broken up into five depth intervals

TABLE II—Computation Scheme for Dynamic Height Anomaly Uncertainty for Grand Banks Data

p (decibars)	Δp	R_s	R_δ	$R_\delta \cdot \Delta p$
0				
25	25	0.20	0.00015	0.00375
200	175	1.00	76	13300
300	100	0.20	15	1500
400	100	0.10	8	1000
1000	600	0.05	4	3000
				$R_D = 0.19175$

with an approximately constant R_s. The computation may then be made according to the scheme in Table II. From the results given in this table it is concluded that the probable error introduced into the dynamic height by trying to compute it with the use of the *T-S* correlation for the Grand Bank area would be excessive, about $\pm$ 0.05 meters.

An example showing the other extreme is found by determining, for purposes of illustration, the dynamic height of the 300 decibar surface above the 1000 decibar surface in the Sargasso Sea where the *T-S* correlation (2) is an extremely good one. The computation is given in Table III. The total range of uncertainty in dynamic height

TABLE III—Computation Scheme for Dynamic Height Anomaly

p (decibars)	Δp	R_s	R_δ	$R_\delta \cdot \Delta p$
300				
400	100	0.12	0.00010	0.01000
1000	600	0.01	6	3600
				$R_D = 0.04600$

is of the order of 0.046 meters, and the probable error would then be $\pm$ 0.012 meters, which is good.

3. In those cases where the use of the *T-S* diagram for dynamic computations seems feasible (after a preliminary examination using the method in Section 2) a considerable simplification of the actual calculations is possible by constructing special tables for each water mass. These new tables would give the specific volume anomaly δ as a sum of only two terms, so that

$$\delta = [\tau] + [\tau, \gamma] .$$

An example of such tables appears in Section 5. The term $[\tau]$ includes the usual terms δ_s, δ_τ and $\delta_{s,\,\tau}$, whereas the term $[\tau, \gamma]$ includes $\delta_{s,\,p}$ and $\delta_{\tau,\,p}$. It is also possible to include a column, in the table for $[\tau]$, which would give the probable error in δ due to the uncertainty involved in using the *T-S* curve. The accumulation of the errors may then be carried through by integration over depth, just as δ is integrated, and a more accurate estimate of the error will result than can be obtained through the use of Table I.

4. The range of uncertainty R_s in the salinity for a given temperature may arise from the following causes:

a. R_s will be very large wherever the slope of the *T-S* curve is small, as is the case in Baffin Bay water.

b. R_s will be large whenever seasonal variations and mixing occur. These conditions predominate, for example, near the surface.

c. Measurements of T and S at any station are made only for certain discrete values of the depth. Even if the precision of individual discrete measures were indefinitely high, an error would still be introduced due to the assumption that the specific volume varies linearly or "smoothly" between the points where the measures are made. Indeed, most recent experience with the bathythermograph indicates a wide prevalence of very irregular variations.

d. The accuracy of individual salinity measurements used in drawing up the T-S curve is limited, which fact implies an interesting point about the use of the T-S curve, since there may be an advantage in using the T-S curve for bodies like the Sargasso Sea instead of using individual measures. The value of R_s in the Sargasso Sea water below 300 meters is so small that it is possible that it arises from the inaccuracies of the salinity determinations themselves rather than from actual fluctuations in the composition of the water mass. In such a case the use of the T-S diagram would be more accurate than the use of individual measures for dynamic current computations.

5. In order to see how these ideas work out in practice, the following example has been prepared from "Atlantis" Stations 1637–1642 across the Gulf Stream at Onslow Bay. The T-S curve for this section shows that it is an intermediate case; it is not as scattered as in the case of the Grand Banks, but on the other hand, it is not as ideal as the one for the deep Sargasso Sea.

First, the anomaly of the dynamic height was computed by using the standard tables of Bjerknes and Sandstrom (1), from the formula

$$\delta = \delta_s + \delta_T + \delta_{s,\,T} + \delta_{s,\,P} + \delta_{T,\,P},$$

and by summing over the first 1000 meters of depth. The summations for stations 1637–8 were carried only for the entire depth to the ocean bottom, since in each of these instances the ocean depth is less than 1000 meters. This value of the dynamic height anomaly for each station is indicated in Table IV.

A T-S diagram for these six stations was then constructed, and a mean curve drawn. Both S and R_s were scaled off as functions of T; the results appear in Table V. Using this table and the Bjerknes-Sandstrom tables (1), special tables (as described above in Section 3) were constructed for this water mass, and these are included here as Tables VI and VII. Specific volume anomalies were then computed from Tables VI and VII and summed over the first 1000 meters. The resulting dynamic height anomalies appear in Table IV.

TABLE IV—Comparison of Dynamic Height Anomalies of "Atlantis" Onslow Bay Stations as Computed by the Standard Tables of Bjerknes and Sandstrom and Those by the Special Tables VI and VII

(1) "Atlantis" Station Number	1639	1640	1641	1642	1637	1638
(2) Reference Level (meters)	1000	1000	1000	1000	189	461
(3) Dynamic height anomaly (meters) as computed by standard tables	1.690	1.756	1.711	1.472	0.473	1.027
(4) Dynamic height anomaly (meters) computed from Tables VI and VII	1.713	1.834	1.746	1.527	0.459	1.035
(5) Differences: (4) − (3) (meters)	0.023	0.078	0.035	0.055	−0.014	0.008

TABLE V—The *T-S* Relation for Onslow Bay, Including the Range of Uncertainty of Salinity

Temperature	*Salinity*	*Uncertainty of Salinity*
T	S	R_s
27.5	36.00	0.20
25.0	36.15	.20
22.5	36.35	.40
20.0	36.45	.30
17.5	36.40	.05
15.0	35.95	.05
12.5	35.62	.05
10.0	35.20	.04
7.5	35.08	.04
5.0	35.06	.04
2.5	35.04	.04

A comparison of the dynamic height anomalies, as computed by the standard technique and those computed by Tables VI and VII, shows (Table IV) that a considerable deviation exists between the results computed by the two different methods. This must be due to a variation of the water composition within the mass that was chosen. However, if the stations are divided into two groups—stations 1637–8, and stations 1639–42, the mean difference of the first group is negative, and that of the second group is + 0.047 meters. This suggests that there is a real change of water mass from one group to the other. As

TABLE VI—Special Onslow Bay Table of the Correction [τ]

T	[τ]	T	[τ]
27	0.00438	14	0.00122
26	404	13	112
25	370	12	105
24	336	11	99
23	302	10	94
22	270	9	81
21	241	8	71
20	212	7	60
19	189	6	48
18	166	5	37
17	150	4	27
16	142	3	19
15	132	2	9

TABLE VII—Special Onslow Bay Table of the Correction [τ, p]

p \ T	2½	5	7½	10	12½	15	17½	20	22½	25	27½
decibars	0	0	0	0	0	0	0	0	0	0	0
100	1	1	2	2	3	3	3	3	4	4	4
200	1	2	3	4	5	6	7	8	7	8	8
300	2	4	5	7	8	8	11	11	12	12	12
400	2	5	6	9	11	13	14	15	16	17	17
500	3	6	8	11	13	16	17	18	19	20	21
600	4	7	10	13	16	18	20	22	23	24	25
700	4	8	12	15	18	21	23	25	26	28	29
800	5	10	13	17	21	24	26	29	30	32	33
900	6	11	15	19	23	27	30	33	34	36	37
1000	6	12	17	21	26	30	33	36	38	39	41

a matter of fact, this may be seen from an examination of the T-S curve, where station 1637 differs most widely from the mean distribution. Had 1637 and 1638 been omitted from the construction of the T-S curve, the agreement of the two methods for the remaining stations would have been much better. The probable error of dynamic height anomaly in using the short tables instead of the standard tables for stations 1639–42 (omitting 1637–8 from the correlation diagram) would be about $\pm$ 0.02 meters. It is interesting to compare this probable error with that arising from the salinity measurements themselves. The error in the salinity measurements from these stations is estimated by Iselin (2) to be about $\pm$ 0.02 °/₀₀ as a maximum. To this salinity error there corresponds a maximum error in dynamic height anomaly of about $\pm$ 0.02 meters.

As a result it appears that in certain restricted regions the *T-S* diagram may be used for rough dynamic computations. For more detailed survey work where great accuracy of the result is desired the method using the *T-S* diagram is clearly unsuitable.

6. It is certain that if more soundings were available for each of the stations there would have been more accurate values of dynamic height anomaly. However, there are only a certain number, and therefore there is little *a priori* reason to assume any particular kind of interpolation between these points. Some idea can be obtained of the inaccuracies introduced through a linear interpolation by omitting alternate soundings. For this purpose the data for each station were split into two sets of alternate soundings, and the dynamic height anomalies were computed for these as though they were the only data available in each case. The results, using the standard tables (1), are given in Table VIII, along with the differences between these values

TABLE VIII. Error Due to Using a Linear Interpolation between Soundings as Indicated by Splitting the Soundings for Each Station into Two Alternate Sets

(1) "Atlantis" Station	1639	1640	1641	1642
(2) Dynamic height anomaly from complete data (meters)	1.690	1.756	1.711	1.472
(3) Dynamic height anomaly from first half of soundings taken alternately	1.711	1.803	1.754	1.453
(4) Dynamic height anomaly from second half of soundings taken alternately	1.707	1.765	1.698	1.429
(5) Difference: (3) − (2)	0.021	0.047	0.043	−0.019
(6) Difference: (4) − (2)	0.017	0.009	−0.013	−0.043

and the values computed from the complete data. In all cases it is seen that the dynamic height anomalies as computed by the two methods are considerably different—of the order of accuracy in which we are interested. It is essential to recognize, therefore, that the values in which all the data are used are subject to errors nearly of the same (though somewhat smaller) magnitude. This source of error—the interpolation error—appears in addition to the other errors. However, it is possible to eliminate the interpolation error almost completely from the dynamic height computations if use is made of a bathythermogram in conjunction with the more exact bottle data.

It would be unwise to claim too much for the techniques proposed in this note. However, it may be possible (for certain very homogeneous water masses such as the Sargasso Sea), by judicious use of the *T-S* correlation curve, the bathythermogram, the usual bottle samples and temperatures, that errors due to both individual measurements of salinity and interpolation may be largely suppressed, with the result that the dynamic heights so obtained would be certain to an additional half decimal place or better.

ACKNOWLEDGMENT

There is very little which is original with the writer in the present note, since it is the result of the thoughts of a number of people. The possibility of using the *T-S* diagram for dynamic computations was first mentioned to the writer by Dr. C.-G. Rossby. From subsequent correspondence it appears that Mr. C. O'D. Iselin and Mr. Floyd Soule had considered the idea years ago. An estimate of the desired accuracy in work of this kind was obtained from some unpublished notes of Dr. R. B. Montgomery. In addition, the writer has had the opportunity to discuss these and related matters with Messrs. Frederick Fuglister, V. P. Starr and A. C. Vine.

REFERENCES

1. Bjerknes, V. and J. W. Sandstrom
   1910. Dynamic meteorology and hydrography. Pt. I. Statics. Publ. Carneg. Instn., No. 88: 1–68.
2. Iselin, C. O'D.
   1936. A study of the circulation of the western North Atlantic. Pap. phys Oceanogr. Meteorol., *4* (4): 6.
3. Soule, F. M.
   1940. International ice observation and ice patrol service in the North Atlantic Ocean. Bull. U. S. Cst. Guard, No. 30: 36–40.
4. Sverdrup, H. U.
   1933. Vereinfachtes Verfahren zur Berechnung der Druck- und Massenverteilung im Meere. Geofys. Publ., *10* (1): 1–9.

NOTES ON THE DISTRIBUTION OF ENERGY AND FREQUENCY IN SURFACE WAVES

By

C.-G. Rossby

The University of Chicago

The behavior of irrotational surface waves of small amplitude in deep water has been thoroughly investigated through theoretical studies extending over a period of more than one hundred years. Waves of this type are therefore particularly well suited for demonstration of the characteristics of energy and frequency distribution and propagation in dispersive media. In the present note a few comments will be made on the distribution of energy with respect to frequency in such waves.

A. *On the energy spectrum of waves emanating from a point source.*

In a recently published paper (Rossby, 1945) the author has derived a general equation relating frequency (ν) and wave number (k) in progressive plane waves. If the x-axis represents the direction of propagation of the waves, one finds

$$\frac{\partial \nu}{\partial x} + \frac{\partial k}{\partial t} = 0 . \tag{1}$$

The derivation of this equation is based on the assumption that wave crests are conserved and that ν and k are slowly varying functions of x and t.

If the physical theory for the particular wave motion under investigation leads to a relation between ν and k so that

$$\phi (\nu, k) = 0 , \tag{2}$$

or

$$c = F (L) , \tag{3}$$

where c is the phase velocity and L is the wave length, it follows that (1) may be written in the form

$$\frac{\partial \nu}{\partial t} + c_g \frac{\partial \nu}{\partial x} = 0 , \tag{4a}$$

or

$$\frac{\partial c_g}{\partial t} + c_g \frac{\partial c_g}{\partial x} = 0 , \tag{4b}$$

where

$$c_g = c - L\frac{dc}{dL} = \frac{d\nu}{dk} \tag{5}$$

is the group velocity.

If the energy per unit area (or unit length along the axis of wave propagation) is designated by E, it is normally assumed that the energy propagation obeys the law

$$\frac{\partial E}{\partial t} + \frac{\partial}{\partial x} c_g E = 0\,. \tag{6}$$

This equation is usually interpreted to mean that energy is propagated with the group velocity. A less restrictive interpretation, and formally equally correct, is to state that the flux of energy across consecutive planes moving with the group velocity does not vary from plane to plane. Such an interpretation would obviously imply that energy may be transferred from one end of the wave train to the other, or that, if the distribution of frequency with respect to x at all times is monotone, energy may be transferred from one end of the energy spectrum to the other.

If ν is a monotone function of x, but varying with time, it is possible to introduce a specific energy per frequency interval, so that

$$E_\nu \delta\nu = \pm E\delta x\,. \tag{7}$$

In that case (6) changes into

$$\frac{\partial}{\partial t}\left(E_\nu \frac{\partial \nu}{\partial x}\right) + \frac{\partial}{\partial x}\left(E_\nu c_g \frac{\partial \nu}{\partial x}\right) = 0\,, \tag{8}$$

or, because of (4a),

$$\frac{\partial E_\nu}{\partial t} + c_g \frac{\partial E_\nu}{\partial x} = 0\,. \tag{9}$$

It follows through comparison of (4a) and (9), that the Jacobian $\dfrac{\partial(E_\nu, \nu)}{\partial(x, t)}$ vanishes and hence,

$$E_\nu = f(\nu)\,. \tag{10}$$

Thus the spectral distribution of E_ν is independent of time. It is obvious that instead of (10) one may substitute an equation of the form

$$E_\lambda = \phi(\lambda)\,, \tag{11}$$

where $\phi(\lambda)$ likewise is independent of time.

Cauchy and Poisson[1] have investigated the surface wave trains generated when an elevated strip along the line $x = 0$ is permitted to seek equilibrium. The elevation of the free surface η is originally concentrated near the point $x = 0$ and

$$\int_{-\infty}^{+\infty} \eta \delta x = 1. \tag{12}$$

Two wave trains are generated, moving along the positive and negative x-axes away from the point source. On the positive x-axis the resulting wave train is given by the asymptotic solution

$$\eta = \sqrt{\frac{g}{8\pi}} \frac{t}{x\sqrt{x}} \left(\cos \frac{gt^2}{4x} + \sin \frac{gt^2}{4x} \right). \tag{13}$$

The frequency of these waves is given by

$$\nu = \frac{gt}{2x}, \tag{14a}$$

the wave length λ by

$$\lambda = \frac{8\pi x^2}{gt^2}, \tag{14b}$$

and the group velocity by

$$c_g = \frac{x}{t}. \tag{15}$$

The amplitude is given by

$$\eta_o = \sqrt{\frac{g}{8\pi}} \frac{t}{x\sqrt{x}}, \tag{16}$$

and since

$$E = \frac{g\rho\eta_o^2}{2}, \tag{17}$$

it follows that

$$E = \frac{\rho g^2 t^2}{16\pi x^3}. \tag{18}$$

From the relation

$$E_\lambda \delta\lambda = E\delta x, \tag{19}$$

one finds

$$E_\lambda = \frac{\rho g^3 t^4}{256\pi^2 x^4} = \frac{\rho g}{4\lambda^2}, \tag{20a}$$

and the energy spectrum is therefore independent of time, as indicated in (11). A dimensional constant, measuring the original cross-sec-

[1] For a summary of the investigations of Cauchy and Poisson, see Lamb (1932).

tional area of the elevated portion of the sea surface has been suppressed through the introduction of condition (12), and thus equation (20a) is dimensionally incorrect, but this obviously does not effect the main result, the invariance of $E_\lambda(\lambda)$ with time. It is perhaps worth noting that by means of the transformation

$$E_\nu \delta\nu = -E_\lambda \delta\lambda, \tag{20b}$$

one obtains

$$E_\nu = \text{constant} \cdot \nu. \tag{20c}$$

The results obtained above suggest that energy cannot be transferred from one frequency to another. To explore this point, it is desirable to investigate the time rate of the establishment of the energy spectrum given in (20a).

It is obvious from the asymptotic solution given above, or from the exact solution,

$$\eta = \frac{\sqrt{g}\,t}{\pi x\sqrt{x}} \int_0^\omega \cos(\zeta^2 - \omega^2) d\zeta, \qquad \left[\omega = \sqrt{\frac{gt^2}{4x}}\right], \tag{21}$$

that the longest, fully developed wave observed at any one time corresponds to a fixed, low value ($\omega_\circ$) of ω. Thus

$$\frac{gt^2}{4x} = \omega_\circ^2, \tag{22}$$

and, from (14b)

$$\lambda_{\max.} = \frac{\pi g t^2}{2\omega_\circ^2}. \tag{23}$$

Thus, while the asymptotic energy spectrum given in (20a) is independent of time, it follows from (23) that this spectrum is cut off on the low-frequency end; this portion of the spectrum is gradually extended, at an accelerated rate, to lower and lower frequencies (longer and longer wave lengths). A graphical representation of this process is given in Fig. 24.

The energy for this portion of the spectrum must be obtained, either through propagation of energy across planes moving with the group velocity (transfer of energy from higher to lower frequencies), or through the transformation of an initial energy supply into wave energy. In either case, in view of the absence of the low-frequency portion of the spectrum in the early part of the process, it is necessary to assume that some form of energy is transferred, at some time or another during the process, from left to right (toward increasing values of λ) across the group velocity planes.

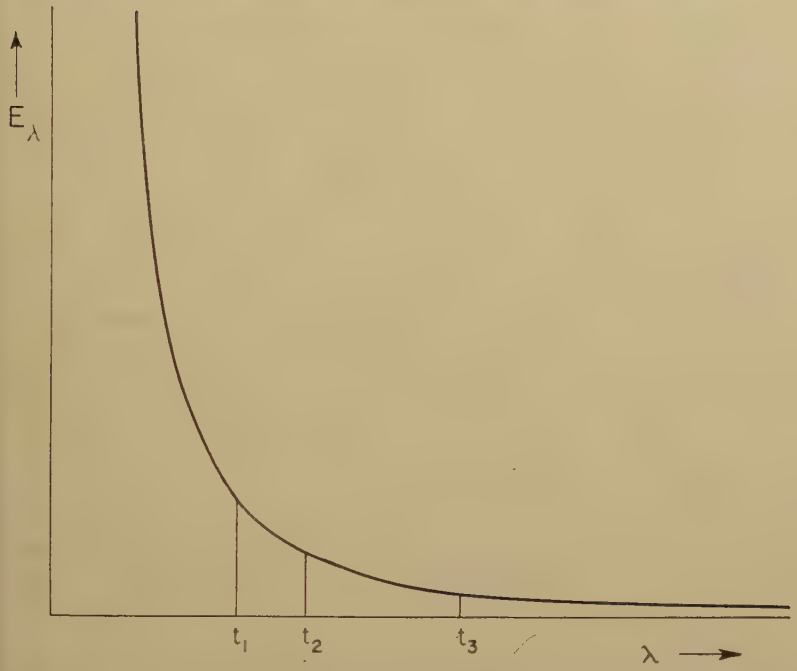

Figure 24. Graphical representation of forward portion of energy spectrum emanating from a point source, and of three successive positions of maximum wave length for fully established wave motion.

To investigate this point further it is helpful to determine the disposition of the original supply of elevated water. We shall compute the total amount of excess water contained at any given time in a unit strip extending from x to infinity.

One finds, from (21)

$$\int_x^\infty \eta dx = \frac{\sqrt{g}}{\pi} \int_0^\infty \frac{t dx}{x\sqrt{x}} \int_0^\infty \cos(\zeta^2 - \omega^2)\, d\zeta, \tag{24}$$

and, from the definition of ω in (21),

$$d\omega = -\omega \frac{dx}{2x}. \tag{25}$$

Hence

$$\int_x^\infty \eta dx = \frac{4}{\pi} \int_0^\omega d\omega \int_0^\omega \cos(\zeta^2 - \omega^2) d\zeta. \tag{26}$$

If one designates, in a manner convenient for our purposes, but departing from standard usage,

$$C(\omega) + iS(\omega) = \int_0^{\omega} e^{i\zeta^2} d\zeta, \tag{27}$$

where C and S are Fresnel integrals, it follows that

$$\int_0^{\infty} \cos(\zeta^2 - \omega^2) d\zeta = C(\omega)\cos\omega^2 + S(\omega)\sin\omega^2 = C\frac{dC}{d\omega} + S\frac{dS}{d\omega}, \tag{28}$$

and hence

$$\int_x^{\infty} \eta dx = \frac{2}{\pi}\int_0^{\omega} \frac{d}{d\omega}(C^2 + S^2) d\omega = \frac{2}{\pi}\left[C(\omega)^2 + S(\omega)^2\right]. \tag{29}$$

Thus the left boundary of the strip containing any given percentage of the amount of elevated water moves along a curve,

$$\frac{gt^2}{4x} = \omega^2 = \text{constant}, \tag{30}$$

with uniformly accelerated speed (Fig. 25).

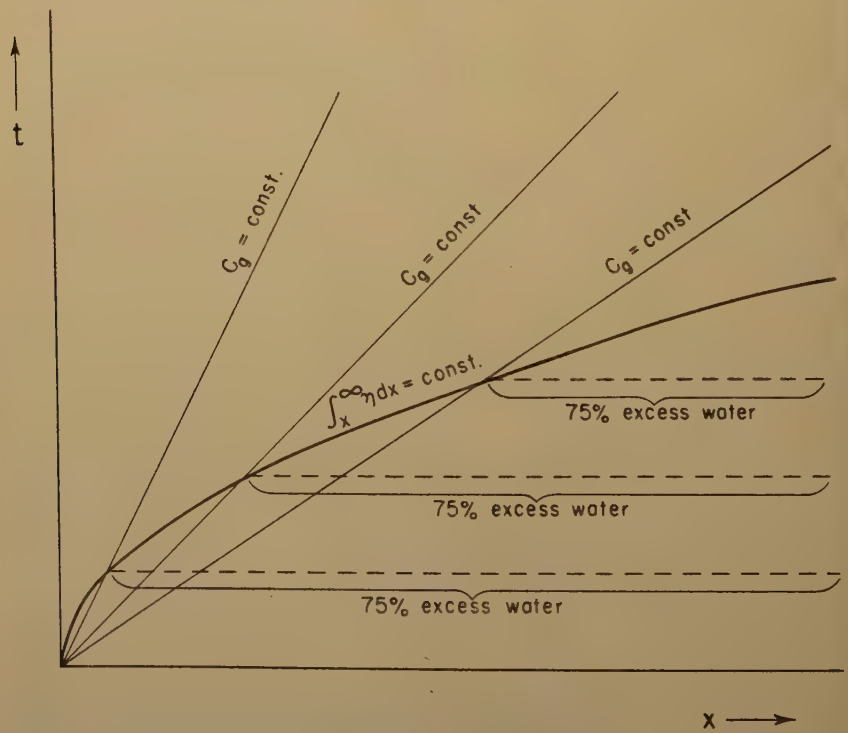

Figure 25. Graphical representation of the sinking and spreading out of excess water mass responsible for the wave motion.

Thus, the elevated water, which obviously represents the source of energy for the wave motion, moves across the group velocity planes at increasing speed. At the same time it spreads out over ever larger areas.

For $x = 0$ one finds that ω becomes infinitely large and thus

$$\int_0^\infty \eta dx = \frac{2}{\pi}\left[C_\infty^2 + S_\infty^2\right] = \frac{1}{2}, \tag{31}$$

as should be expected, but this asymptotic value is practically reached already for ω_0 values corresponding to the first fully developed wave. One may conclude that at any time during the establishment of the energy spectrum given in (20a) there is a temporary flux of potential energy which has not yet broken down into wave energy, across the group velocity planes and into the low frequency part of the spectrum. Part of this potential energy is left behind as wave energy, but the remainder travels on, at accelerated speed, to establish wave motion of even lower frequency.

It should be added that the basic assumption of small amplitudes is most likely to be satisfied in the low-frequency part of the energy spectrum with which the above analysis deals.

B. *On apparent increases in period resulting from convergent group velocity distributions.*

The general integral of equation (4b) in the preceding section is

$$c_g = f(x - c_g t), \tag{32}$$

or

$$x = c_g t - \phi(c_g), \tag{33}$$

where f and ϕ are arbitrary. In the case of point sources of energy, where no impressed frequencies need to be considered,

$$x = c_g t, \tag{34}$$

represents a typical solution. One may now attempt to generalize (34) by assuming a solution of the form

$$c_g = \frac{x}{t} F\left(\frac{gt^2}{4x}\right), \tag{35}$$

the parameter $\frac{gt^2}{4x}$ being nondimensional. The function F may be determined through substitution in (4b). Another technique, which leads to similar results, is to deal with (33). From dimensional considerations one should expect that

$$\phi(c_g) = \pm s_\circ \frac{c_g^2}{g}, \tag{36}$$

g being the only prescribed dimensional constant. Here $s_\circ$ is a nondimensional, positive constant. Substitution in (33) gives

$$x = c_g t \pm s_\circ \frac{c_g^2}{g}. \tag{37}$$

For $t = 0$ one obtains

$$x = \pm s_\circ \frac{c_g^2}{g}. \tag{38}$$

The upper sign pertains to an initial group velocity distribution, beginning with

$$c_g = 0\,, \qquad \text{for } x = 0\,, \tag{39}$$

corresponding to short wave lengths, and proceeding to very long waves for large positive x-values. This form of (37) represents a divergent group velocity distribution and is of no interest to us in the present analysis. The lower sign gives, for $t = 0$,

$$x = -s_\circ \frac{c_g^2}{g} \tag{40}$$

or an initial distribution of progressive waves, of vanishing wave length near $x = 0$ and becoming increasingly large for large negative x-values. Since the longer waves travel faster than the shorter, the corresponding group velocity planes must converge and thus give rise to an increase in energy per unit area.

The intersection of two adjacent group velocity lines is obviously obtained, in form (33), as the intersection of

$$x = c_g t - \phi(c_g)\,, \tag{41a}$$

and

$$x = (c_g + \delta c_g)t - \left(\phi + \frac{d\phi}{dc_g}\delta c_g\right). \tag{41b}$$

Thus, in our special case the parametric equation for the curve of intersection is given by (Fig. 26)

$$x = c_g t - s_\circ \frac{c_g^2}{g}, \tag{42}$$

and

$$0 = t - \frac{2 s_\circ c_g}{g}. \tag{43}$$

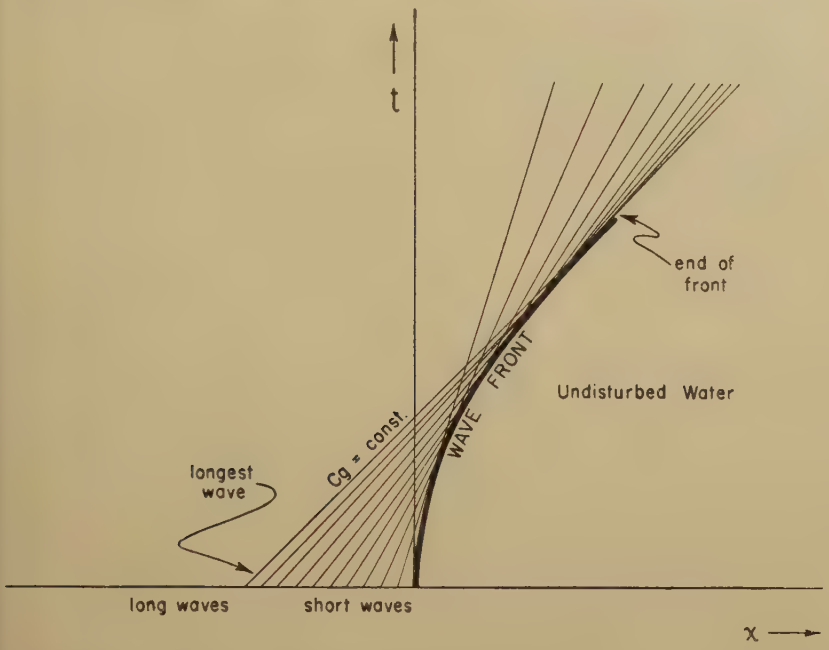

Figure 26. Formation of wave front as a result of a convergent group velocity distribution. Period of wave motion in front increases with time.

Elimination of c_g gives

$$x = \frac{gt^2}{4s_0}. \tag{44}$$

In the region

$$x \geqslant \frac{gt^2}{4s_0}, \tag{45}$$

the water will be undisturbed. On the line given by (44) a strong concentration of wave energy is suddenly encountered. The larger the value of x (or t), the further from the rear of the original wave train will be the source of the energy, and hence, the longer will be the period.

The variation of period with time is obtained from (43), which gives

$$c_g = \frac{g}{2\nu} = \frac{gT}{4\pi} = \frac{gt}{2s_0}, \tag{46}$$

and thus the period appears to increase with time. *It should be emphasized that the curve given in (44) cannot be extended beyond the maxi-*

mum period T for which energy is available in the original wave train. The process indicated above represents a concentration of energy available in a given frequency belt but does not lead to generation of energy in frequency regions where none was available originally.

It should be added that the nondimensional constant s_0 has a simple physical interpretation. It follows from (40) that in the initial state,

$$c_g = \sqrt{\frac{-gx}{s_0}} = \frac{gT}{4\pi}, \tag{47}$$

and since

$$L = \frac{gT^2}{2\pi}, \tag{48}$$

one finds

$$-\frac{x}{s_0} = \frac{L}{8\pi}, \tag{49}$$

or

$$\frac{dL}{d(-x)} = \frac{8\pi}{s_0}. \tag{50}$$

Thus $1/s_0$ is proportional to the constant space gradient of the wave length in the initial wave train.

The group velocity distribution given in (37) corresponds to one obtained independently by W. Munk using a different method and recently communicated to the author by letter.

SUMMARY

In the first section of this paper an attempt is made to determine the source of the wave energy in the long-wave forerunner of a train of plane surface gravity waves emanating from a point source. It is shown that the amount of energy $E_\lambda d\lambda$ contained between the wave lengths λ and $\lambda + d\lambda$ is independent of time. Thus there is no transfer of wave energy from one portion of the spectrum to another. It may be shown, however, that the elevated water mass which originally was concentrated at the point source of the wave motion rapidly spreads out and sinks, its potential energy being converted into wave energy. Thus the successive establishment of wave energy E_λ for larger and larger values of λ may be interpreted as the result of a rapid and transient transport of potential energy outward, a small portion of this potential energy supply being converted into wave energy in each successive spectral region.

In the second part of the paper it is shown that a train of progressive surface waves, in which the group velocity of the forward portion is less than that of the rear portion, may give rise to the formation of a sharp progressive wave front, in which the wave period increases with time. This wave front may be given in parametric form as a special solution of the equation for the propagation of group velocity, c_g, namely,

$$\frac{\partial c_g}{\partial t} + c_g \frac{\partial c_g}{\partial x} = 0 .$$

REFERENCES

LAMB, HORACE
1932. Hydrodynamics. 6th ed. Cambridge Univ. Press. p. 384.
ROSSBY, C.-G.
1945. On the propagation of frequencies and energy in certain types of oceanic and atmospheric waves. J. Meteorology, *2* (4): 187–204.

A THEORETICAL ANALYSIS OF THE ZOOPLANKTON POPULATION OF GEORGES BANK[1]

By

Gordon A. Riley

Woods Hole Oceanographic Institution
and the
Bingham Oceanographic Laboratory

Studies by Fleming (1939), Riley and Bumpus (1946), and Riley (1946) of the seasonal variations of marine phytoplankton populations have resulted in the development of a growth budget in which the rate of change of the population is balanced against the rates of all the processes that increase or decrease the organic content of the population. The fundamental basis of this type of analysis is a differential equation in which the rate of change of the carbon content of the phytoplankton at any time is equal to the difference between the rate of accumulation of carbon by photosynthesis and the rates of dissipation by respiration, grazing, and natural death. Furthermore, since interest is centered in the seasonal cycle rather than long period fluctuations, it is assumed for practical purposes that over a period of one year the sum of the variations expressed by the equation is equal to zero. In the first two papers cited above, a study was made of the period of the spring diatom flowering in the Georges Bank area of the Gulf of Maine and in the English Channel where the budgets proved useful in describing quantitatively the phytoplankton-zooplankton grazing relationship. In the third paper, a more elaborate but somewhat empirical treatment of the same general type was used to evaluate the entire yearly phytoplankton cycle on Georges Bank.

The advantage of this method is that the balancing of the budget permits an estimate of the overall accuracy of the results. It is therefore a useful tool in putting ecological theories to a quantitative test. The disadvantage is that it requires detailed quantitative information about many processes, some of which are only poorly understood. Therefore, until more adequate knowledge is obtained, any application of the method must contain some arbitrary assumptions and many errors due to over-simplification.

This type of treatment is not necessarily limited to phytoplankton studies. Any population that is ecologically homogeneous may be

[1] Contribution No. 368 from the Woods Hole Oceanographic Institution.

considered in an analogous way. For example, the animals which live by grazing on phytoplankton may be analyzed by an equation such as:

$$\frac{dH}{dt} = H(A\text{-}R\text{-}C\text{-}D)\,, \qquad (1)$$

in which:

H = the herbivore population;
A = the rate of assimilation of food by the herbivores;
R = their respiration rate;
C = the rate of consumption of herbivores by their predators;
D = the herbivore death rate.

Then the size of the population at the end of time t is determined by the equation:

$$H_t = H_o e^{(A-R-C-D)t}. \qquad (2)$$

While the theory is simple enough, the practical application is full of uncertainty because we know so little about the physiology of herbivores and about their predators. The writer feels that it is worthwhile to include such an analysis in the general study of Georges Bank plankton, but the available information is only a small fraction of what is needed for the work, and the results are therefore to a large degree speculative.

The data in the present analysis are derived largely from the two papers referred to previously. The zooplankton population on Georges Bank, shown in Fig. 27, was estimated as grams of carbon per m^2 of sea surface, determined by applying a conversion factor to the measurements of zooplankton volume. Herbivores constitute the main bulk of the zooplankton. Since there is no simple and accurate method of quantitatively allowing for that part of the zooplankton which is carnivorous, it will be assumed that the population of herbivores is equal to the total zooplankton.

Assimilation. The assimilation rate is strictly defined as grams of carbon taken into the herbivore tissues (and therefore available for growth or energy) per day per gram of carbon in the herbivore population. Since the assimilation rate does not readily lend itself to quantitative measurement, it is necessary to use indirect evidence to derive a practical definition which is at best an approximation. This definition is as follows:

The assimilation rate is 0.0075 P, where P represents grams of phytoplankton carbon per m^2, except when this value exceeds 8 per cent of the animals' weight per day, which is set as the maximum limit of the assimilation rate.

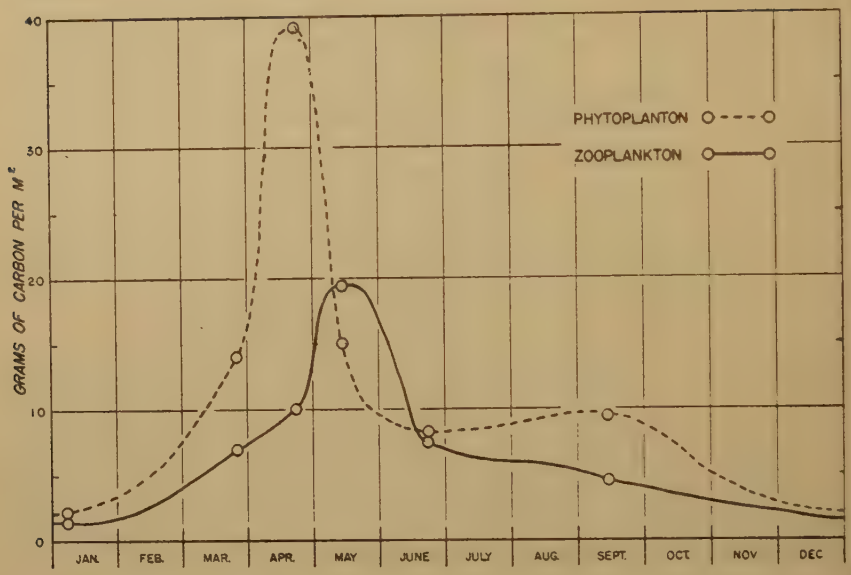

Figure 27. Seasonal cycles of phytoplankton and zooplankton on Georges Bank.

The definition is based on the following line of reasoning: It is generally believed that a unit quantity of zooplankton filters the food from a constant volume of water per unit time and therefore eats a constant fraction of the phytoplankton population per day irrespective of the absolute size of the population. This presupposes that the feeding rate is not affected by seasonal changes in temperature, which may not be strictly true, although previous discussion of the subject (Riley, 1946) indicated that on Georges Bank the feeding rate was probably independent of temperature. In the paper just referred to, it was estimated that the fraction of the phytoplankton consumed by a unit quantity of zooplankton (1 g. carbon per m^2) was 0.0075. Therefore, the daily rate of consumption of food by herbivores is 0.0075 P, where P represents grams of phytoplankton carbon. The phytoplankton population is shown in Fig. 27, and the consumption rate derived from it is the upper curve in Fig. 28A.

In a study of the plankton of the English Channel, Harvey,Cooper, Lebour and Russell (1935) concluded that utilization (the ratio of assimilation to consumption) was very near unity through most of the year, but that the spring diatom flowering provided the animals with more food than they could use, so that some was excreted in a semidigested condition. The same thing appears to occur in the

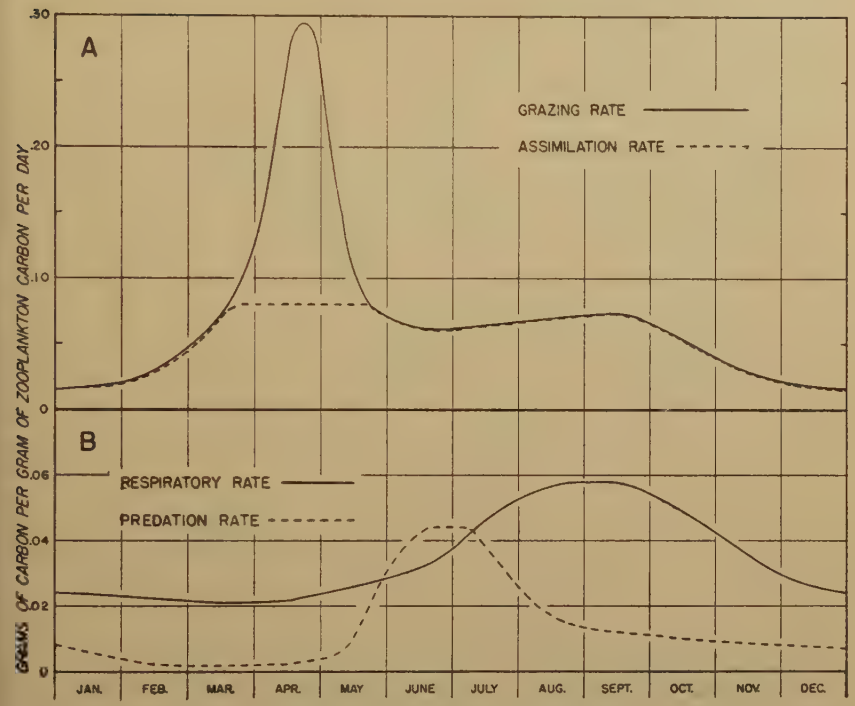

Figure 28. Processes of accumulation and loss of organic matter by Georges Bank zooplankton. A. Estimated rates of consumption and assimilation of phytoplankton food. B, Estimated rates of respiration and consumption of zooplankton by its predators.

Georges Bank area, for although the growth budget for phytoplankton indicates that consumption continues at a constant rate through the spring flowering, the amount consumed is at least twice as much as is needed to account for the observed rate of animal growth. Furthermore, the zooplankton appears to have attained its maximum rate of spring growth in late March before the phytoplankton reached its peak and to have maintained this rate until about the middle of May, when the diatom flowering was largely finished. It seems likely, therefore, that the assimilation rate during the whole of the spring flowering was no larger than the consumption rate of 0.080 observed at the beginning and end of this period. The definition therefore sets 0.080 (8 per cent per day) as the maximum rate of assimilation, and during the remainder of the year it is assumed that assimilation approximately equals consumption. The final result is shown by the broken curve in Fig. 28A.

Respiration. It will be assumed that the respiratory rate increases with an increase in temperature and is not affected by any other factor. Thus

$$R = rf(T)\,, \tag{3}$$

in which:

R = the respiratory rate in g. carbon consumed per g. of herbivore carbon per day;
r = the respiratory rate at 0° C = 0.019 (1.9% of the animals' weight per day);
T = Temperature (°C), the seasonal cycle of which is shown in Fig. 29;
$f(T)$ = the ratio of the respiratory rate at any temperature T to the rate at 0°, as shown in Fig. 29, inset.

This definition is derived from a study of the respiration of the copepod *Calanus finmarchicus* by Marshall, Nicholls and Orr (1935). They found that the increase in the respiratory rate with temperature

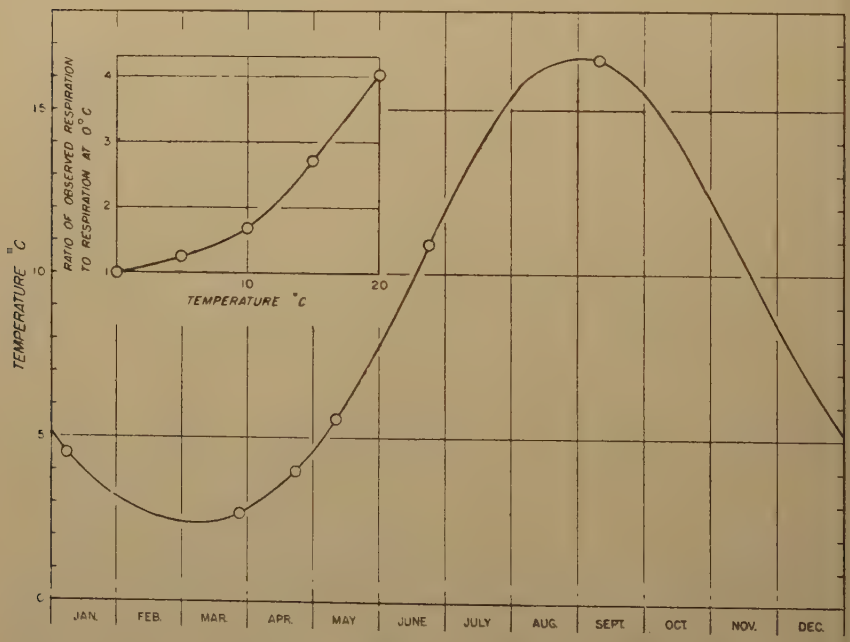

Figure 29. Seasonal temperature change on Georges Bank. Inset, estimated effect of temperature on zooplankton respiration.

did not have an easily defined form such as the van't Hoff law; hence in the present treatment it is necessary to use a graphical definition of the type shown in the inset in Fig. 29. Each point on the curve is

obtained by averaging their experiments with stage *V* copepodites and adult males and females. Using this average curve as a basis, a value for the constant r can now be derived from each of the experiments, regardless of the temperature at which it was conducted. The experiments yield a large range of values, from 0.006 to 0.029, which average 0.019. This average value for the constant is used in the present report. The seasonal change in the estimated respiratory rate is shown in Fig. 28B.

Predation and loss by other causes. It will be assumed that herbivore predators expend a constant feeding effort irrespective of the amount of food available. Then the total amount of food eaten will be proportional to the product of predators and prey, and the rate of consumption of the prey will be proportional to the number of predators. This is similar to the assumption previously made about the phytoplankton-zooplankton grazing relationship, and it leads to an equation such that:

$$C = cS \qquad (4)$$

where:

C = the rate of consumption of herbivores;
c = a constant;
S = the quantity of herbivore predators.

It seems likely that sagittae are the most important herbivore predators in the Georges Bank area, since they are numerically very abundant and since, according to LeBour (1922, 1923), they commonly feed on copepods, although fish larvae and other sagittae also constitute part of their diet. Other predators, such as mackerel, the pelagic young of various other fishes, decapod larvae and jellyfish are much less numerous than the sagittae; moreover, the quantitative aspects of their part in the food chain are very uncertain, and therefore, they are not included in the analysis of predation.

Fig. 30 is the seasonal cycle of *Sagitta elegans*, the only quantitatively important species of sagittae on Georges Bank, based on data published by Clarke, Pierce and Bumpus (1943). The curve shows a minimum point in early spring and a maximum in early or midsummer. The maximum is poorly defined due to the lack of summer data. However, it is clear that the time when the sagittae increased most rapidly coincided with the seasonal peak in total zooplankton, just as the latter increased most rapidly at the time of the diatom flowering. Thus there was a lag period of roughly a month in successive constituents of the food chain.

Little is known about the feeding rate of sagittae, or about the quantity of organic material involved. It is not possible, therefore,

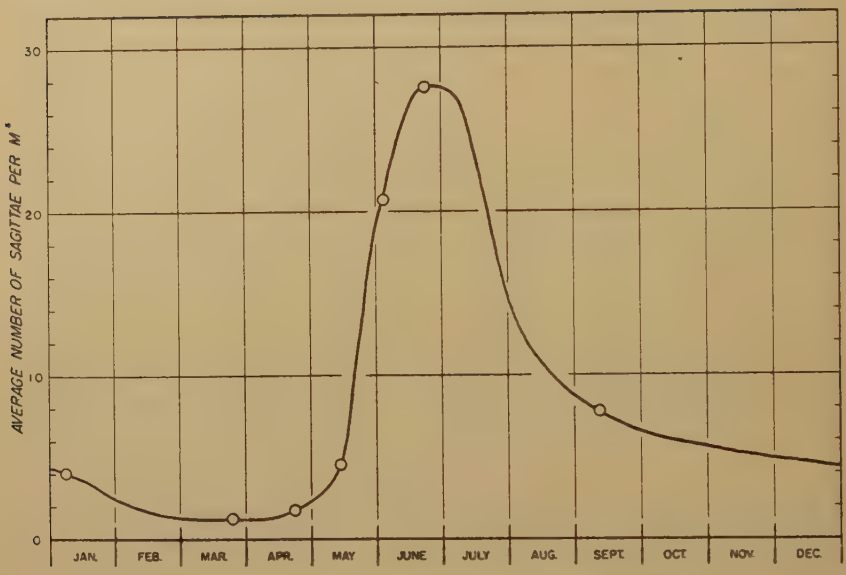

Figure 30. Seasonal change in the concentration of *Sagitta elegans* on Georges Bank.

to assign an experimentally determined value for the constant c in equation (4). An approximation can be obtained by statistical methods as will be shown later. However, it is first necessary to consider the herbivore death rate.

It will be assumed that the death rate D is constant. In this category are lumped several processes, such as natural death, predation by animals other than sagittae, and dilution of the population by water movements. None of these factors is actually constant, with the possible exception of natural death, although there is a slight factual basis in that the net loss is more uniform than any one of its component factors, for predation is certain to be more important during the summer season and loss by water transport more important during the winter.

On the basis of these assumptions, equation (1) is rearranged so that the terms that have already been evaluated are on the left, with predation and death on the right:

$$A - R - \frac{1}{H}\left(\frac{dH}{dt}\right) = cS + D\,.$$

Numerical values for the left-hand side of the equation are determined for various times of the year, and corresponding values for S are read

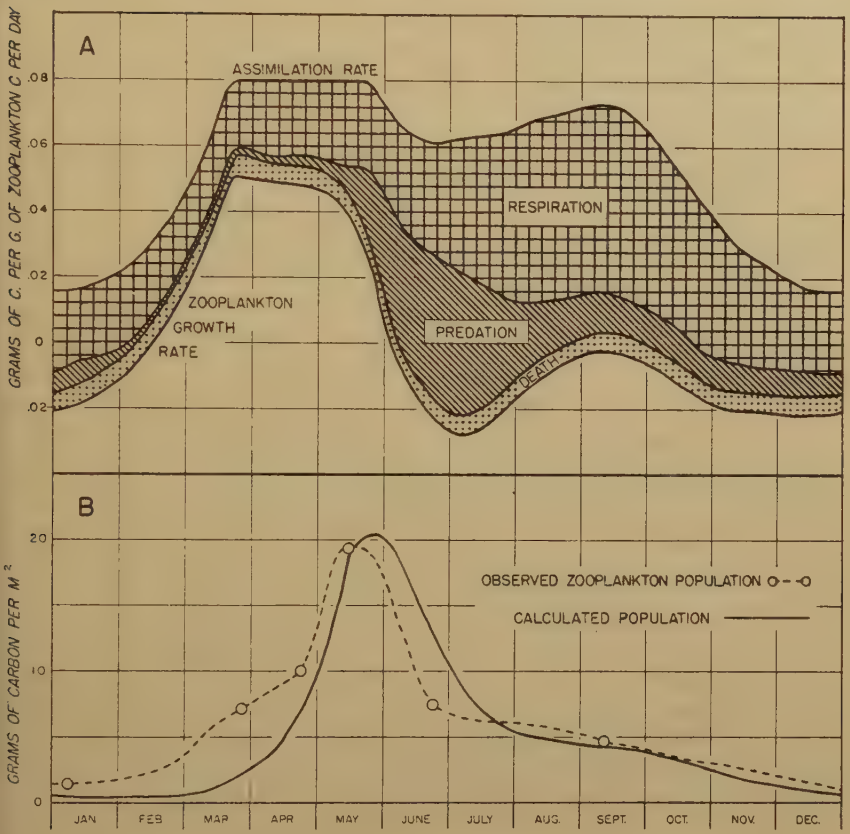

Figure 31. A. Summation of zooplankton growth processes. For complete explanation, see text (p. 111). B. Observed zooplankton seasonal cycle and the theoretical population curve calculated on the basis of seasonal variations in environmental factors.

from the curve in Fig. 30. The constants c and D can then be estimated statistically by the least squares method, and it is found that

$$A - R + \frac{1}{H}\left(\frac{dH}{dt}\right) = 0.0016\,S + 0.006\,,$$

where S is the number of sagittae per m^3.

Seasonal change in the herbivore population. Fig. 31A is a graphical summation of the various factors that are believed to affect the seasonal rate of change of the herbivore population. The upper curve is the estimated rate of assimilation A. When the respiration rate R is sub-

tracted from the assimilation rate, the result is the second curve. From it are subtracted successively the rate of consumption C and the death rate by other causes D, yielding the bottom curve which is the estimated rate of change of the population. This curve can be approximately integrated by assigning a mean value for the rate of change during successive short intervals of time and by applying these mean rates to equation (2). The absolute size of the population, of course, depends on the integration constant H_c, and this constant is arbitrarily chosen so that the average population will approximate the observed one. The results are shown in Fig. 31B, in which the solid line is the theoretical population curve, and the observed population is indicated by dots connected with a broken line. The curves differ in that the ratio of maximum to minimum population is greater in the theoretical curve, and growth in the late winter and early spring is much slower than that of the observed population. Otherwise fair agreement is obtained, and it appears likely that the general mode of attack is correct, although each step in the analysis would be much improved by further study.

SUMMARY

1. A theoretical analysis of the seasonal cycle of zooplankton in the Georges Bank area is presented. An equation is set up in which the rate of change of the herbivore population in respect to time is equal to the difference between the rate of assimilation of organic material by feeding on the phytoplankton and the rate of dissipation by respiration, predation, and loss by various other causes.

2. With the aid of experimental data and statistical procedures, numerical values are assigned to the constants in the equation. It is then possible to construct a theoretical curve for the herbivore seasonal cycle which is in general agreement with the observed population.

3. This type of analysis is particularly useful in plankton work, since it utilizes all the available quantitative information on the biology of a particular group of organisms in a way that permits testing the overall accuracy of the results.

REFERENCES

Clarke, G. L., E. L. Pierce and D. F. Bumpus

1943. The distribution and reproduction of *Sagitta elegans* on Georges Bank in relation to hydrographical conditions. Biol. Bull. Wood's Hole, *85:* 201–226.

Fleming, R. H.

1939. The control of diatom populations by grazing. J. Cons. Explor. Mer., *14* (2)*:* 210–227.

Harvey, H. W., L. H. N. Cooper, M. V. Lebour and F. S. Russell

1935. Plankton production and its control. J. Mar. biol. Ass. U. K., (N S) *20:* 407–441.

Lebour, M. V.

1922. The food of plankton organisms. J. Mar. biol. Ass. U. K., (N S) *12:* 644–677.

1923. The food of plankton organisms. II. J. Mar. biol. Ass. U. K., (N S) *13:* 70–92.

Marshall, S. M., A. G. Nicholls and A. P. Orr

1935. On the biology of *Calanus finmarchicus*. VI. Oxygen consumption in relation to environmental conditions. J. Mar. biol. Ass. U. K., (N S) *20:* 1–28.

Riley, G. A.

1946. Factors controlling phytoplankton populations on Georges Bank. J. Mar Res., *6* (1)*:* 54–73.

Riley, G. A. and D. F. Bumpus

1946. Phytoplankton-zooplankton relationships on Georges Bank. J. Mar. Res., *6* (1)*:* 33–47.

SEASONAL FLUCTUATIONS OF THE PHYTOPLANKTON POPULATION IN NEW ENGLAND COASTAL WATERS[1]

By

Gordon A. Riley

Woods Hole Oceanographic Institution

and

Bingham Oceanographic Laboratory

An analysis of the seasonal phytoplankton cycle of the Georges Bank area of the Gulf of Maine (Riley, 1946) has shown that fluctuations in the population are largely controlled by the seasonal variations of a few environmental factors. An equation was developed in which the rate of change of the population in respect to time was equal to the photosynthetic rate minus the respiratory rate minus the rate of removal of the population by grazing. These rates were in turn evaluated in terms of incident solar radiation, transparency of the water, the depth of the mixed surface layer, the quantity of phosphate, temperature, and the amount of zooplankton.

This type of analysis, introduced by Fleming (1939) and elaborated in the paper referred to above, can be made to serve a variety of purposes in marine biology. It can be applied to zooplankton populations (Riley, 1947) or other ecologically homogeneous groups of organisms. It may also be used to study regional variations in plankton cycles. An approach to this problem is made in the present paper.

Bigelow (1926), Bigelow, Lillick and Sears (1940), and others have noted the considerable differences in seasonal phytoplankton cycles that occur in the waters off the New England coast. The spring flowering is likely to begin any time between January and early March in the shallow coastal waters, in late March or early April on the offshore banks, and in April or May in the continental slope waters and the deep basins of the Gulf of Maine. The spring diatom burst tends to be smaller in coastal areas than in deep water and may be overshadowed by sporadic flowerings in the late summer and autumn. Autumn flowerings are small or nonexistent in the deeper water. And finally, the total variation between maximum and minimum populations is greater in deep water.

The causes of these differences are not immediately apparent. The basic environment is much the same throughout the area, although

[1] Contribution No. 369 from the Woods Hole Oceanographic Institution.

there are small differences that are largely related to the depth of water—differences in transparency, thermal structure, and in the amount and presumably in the availability of nutrient salts. Perhaps these differences are enough to account for the observed variations in phytoplankton cycles, or perhaps species differences or some environmental factors, which are as yet unmeasured, must be considered.

The type of analysis that was made of the Georges Bank plankton provides a mode of attack on this problem. If plankton growth in the various parts of the region is largely dependent on a few commonly measured environmental factors, then an equation that predicts growth in terms of these factors should be equally applicable in any area. If it is not applicable, either the equation is not properly constructed or there is a certain amount of species variability that cannot be analyzed mathematically.

PHYTOPLANKTON OF THE WOODS HOLE AREA

Lillick (1937) published an account of phytoplankton collections made near the western entrance of Vineyard Sound (Lat. 41° 17′ 35″ N., Long. 71° 00′ 00″ W.) during the period from July 1935 to August 1936. The total cell counts shown in Fig. 32 demonstrate a seasonal cycle which is in general typical of New England coastal waters. The phytoplankton studies were accompanied by determinations of temperature, salinity, phosphate, and nitrate, and in addition zooplankton collections were made (Clarke and Zinn, 1937), and the transparency of the water was measured during the period from November 1935 to September 1936 (Clarke, 1938). Altogether it is the most complete survey that has been made in these waters and is in most respects suitable for comparison with the Georges Bank seasonal cycle.

On Georges Bank it was found (Riley, 1946) that the seasonal change in the size of the total population could be determined with a fair degree of accuracy by the equation

$$\frac{dP}{dt} = P\left[\frac{pI_\circ}{kz_1}(1 - e^{-kz_1})\,(1 - N)\,(1 - V) - R_\circ e^{rT} - gZ\right], \qquad (1)$$

in which:

P = phytoplankton population measured as grams of carbon per m²;
p = a photosynthetic constant = g. of carbon produced per g. of phytoplankton carbon per day per average rate of solar radiation;
$I_\circ$ = average daily rate of incident solar radiation in g. cal. per cm² per minute;
k = extinction coefficient for light transmission;

z_1 = maximum depth of the euphotic zone, defined as the depth at which the light intensity is 0.0015 g. cal. per cm² per minute;

$(1 - N)$ = reduction in photosynetic rate caused by nutrient depletion, defined as phosphate concentration at the surface in mg.-at. of P per m³ divided by 0.55 when the concentration is less than 0.55;

$(1 - V)$ = reduction in photosynthetic rate caused by dilution of the population by vertical turbulence, defined as the ratio of z_1 to the depth of the mixed layer when the latter is greater than z_1;

R_o = phytoplankton respiratory rate at 0° C;

r = rate of change of the respiratory rate with temperature, the value of r being set so that the rate is doubled by a ten degree increase in temperature;

T = temperature in degrees Centigrade;

g = rate of reduction of phytoplankton by the grazing of a unit quantity of zooplankton (one gram of zooplankton carbon);

Z = total quantity of zooplankton in grams of carbon per m².

Numerical values for the constants, obtained from various experimental observations, were as follows: $p = 2.5$, $R_o = 0.0175$, $r = 0.069$, and $g = 0.0075$.

Seasonal variations in environmental factors are shown graphically in the papers by Lillick (1937), Clarke and Zinn (1937) and Clarke (1938). Numerical values were read from the curves to be applied to the equation. In several respects the data differed from the Georges Bank survey, occasionally necessitating changes in the method of calculation.

Probably the most significant difference is the fact that the Georges Bank calculation is based on cruise averages and the one for Woods Hole on individual station analyses. Therefore the latter, while it appears to give a very complete picture of the seasonal cycle, undoubtedly contains a certain amount of variation which is not truly seasonal but rather is the result of horizontal movements of variable water masses.

In the second place, the phytoplankton was measured by counting cells rather than by chemical analysis as in the Georges Bank survey. This does not invalidate the application of the equation, since the latter deals with rates of change rather than with absolute quantities. However, the inherent assumption that cell counts are proportional to the total size of the population irrespective of species composition is not fully justified.

In the Georges Bank survey an average seasonal curve was used to obtain radiation values. Clarke (1938) obtained measurements from the Blue Hill observatory, and these are used in preference to the average curve for the area. Clarke also used photometers to measure the extinction coefficient k, which was of course superior to the Secchi

disc measurements made on Georges Bank. These values for I_o and k were used to estimate the depth of the euphotic zone z_1, defined as

$$z_1 = \frac{ln I_o - ln\, 0.0015}{k}, \qquad (2)$$

In a good many cases, however, z_1 was greater than the actual depth of water at the station (30m.). Therefore, it was necessary to modify the definition of the euphotic zone as follows: z_1 = the depth at which the light intensity is 0.0015 g. cal. per cm^2 per minute, or the total depth of water if the latter is less than the former.

Data on temperature and salinity (Clarke, 1938) show that November and early December was the only time in the year when the waters were mixed to a depth greater than that of the euphotic zone. The correction factor $1 - V$ is therefore relatively unimportant.

Evaluation of the nutrient factor $1 - N$ is based on the average phosphate concentration in the upper 15 m. (mean of analyses at 2 m. and 15 m.). This is preferable to using only surface values, since there appears to be considerable variability at the two levels, which is due to water movements rather than to seasonal fluctuation.

The factors considered up to the present—radiation, transparency, the depth of the euphotic zone, vertical turbulence, and phosphate—are combined in the way indicated in equation (1). The result is the estimated photosynthetic rate of the Woods Hole plankton, shown in the appendix under the heading P_h. The remaining terms in the equation each have a single variable. The respiratory rate varies according to the temperature T. The grazing rate depends on the quantity of zooplankton Z. The latter was collected and measured by methods that are not exactly comparable with those of the Georges Bank survey. On Georges Bank, the zooplankton was caught in a quantitative plankton sampler (Clarke and Bumpus, 1940) using a No. 2 net (22 threads to the cm.), and the volume of plankton was measured by the displacement method. In the Woods Hole area, thirty-minute oblique hauls were made with a 1.5 m. scrim net, and the volume of the catch was measured after settling one month. The scrim net had only ten threads per cm., but the threads were large, so that the pores were not much different from those of the No. 2 net. The efficiency of the net was determined by comparison of the catch with samples taken with a pump. Thus the total quantity of large zooplankton is known with some accuracy, but many forms smaller than Stage IV Calanus were lost through the meshes of the net. The amount lost was probably large, since the authors state that the area produces enormous quantities of young *Pseudocalanus minutus*, particularly during the spring months, and evidence of such an in-

crease does not appear in the scrim net catches. Thus there are two incongruities in the comparison: (a) the Woods Hole survey secured a different and probably smaller fraction of the total zooplankton population, and (b) the volume of plankton was measured by a different method. According to Redfield (1941), settling volumes are three to seven times larger than the displacement volume of the same catch. The two errors appear to work in the opposite directions, but how nearly they balance each other cannot be determined from the available data. As a first approximation it will be assumed that they do,

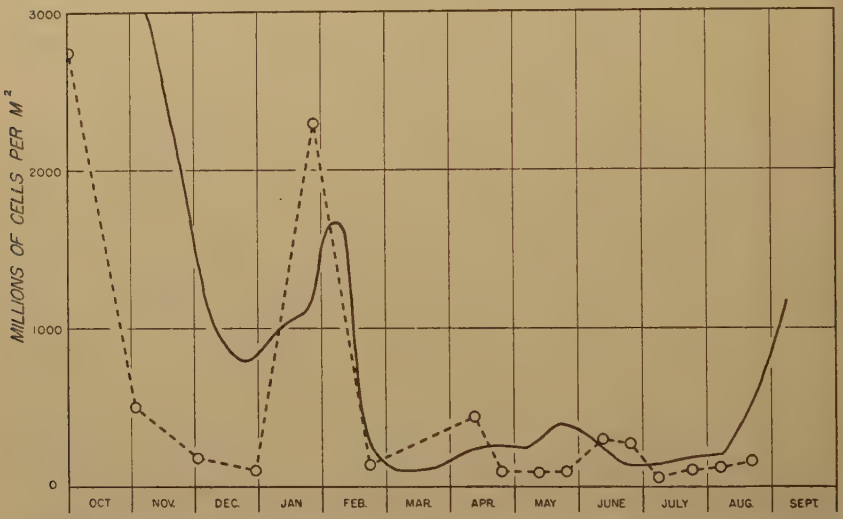

Figure 32. Circles and dotted lines show the seasonal cycle of phytoplankton (millions of cells per m^2) in the waters off Woods Hole. Solid line is a theoretical population curve calculated from environmental factors according to equation (1) in text.

but it will be seen later that the assumption is responsible for considerable uncertainty in the final result.

The appendix shows the estimated zooplankton crop and the derived values for grazing rates. The final steps in the calculation are (a) the determination of the rate of change of the population by subtracting the respiratory and grazing rates from the photosynthetic rate, and (b) the integration of the rate of change of the population in order to obtain the seasonal population curve. This operation is carried out in accordance with methods previously described (Riley, 1946). The result is shown in Fig. 32, in which the calculated population is represented by a solid line, and the observed number of cells by circles and dotted lines.

DISCUSSION

Fig. 32 shows that a fair degree of success is attained in applying the Georges Bank equation to the Woods Hole survey. Although the agreement between the calculated and observed populations is by no means perfect, the equation properly delineates the major points of difference between the phytoplankton cycles in the two areas. The reasons for these differences will be understood more clearly by examination of Fig. 33, which shows a detailed comparison of the various parts of the two calculations. It is apparent from the figure that no one factor is responsible for the results.

During the midwinter lull in plankton production on Georges Bank there is a long period when a close balance exists between accumulation and dissipation of phytoplankton carbon. This period comes to an end when the establishment of vertical stability increases the photosynthetic rate, and the spring diatom flowering follows. In the waters off Woods Hole, where coastal drainage maintains stability, there tends to be an excess of production over consumption as soon as the vernal increase in radiation begins. Probably a flowering may be expected any time after the first of January and is most likely to occur during a period of bright weather.

The quick cessation of the flowering in both areas is a grazing effect. The lack of subsequent spring flowerings of any size in the Woods Hole area is largely the result of nutrient depletion. Differences in the two seasonal cycles appear to be controlled to a considerable extent by the relative availability of nutrients. The deeper water offshore serves as a reservoir of nutrients that are gradually made available to the surface layer by vertical turbulence during the winter and spring months. Hence the total growth in these waters is greater than it is near shore. On the other hand, in the summertime nutrients regenerated on or near the bottom are from time to time returned to the surface layer in the coastal area, leading to sporadic flowerings during the summer and early autumn, while farther offshore the vertical distribution of nutrients seems to be largely confined to the autumn months when increasing turbulence and decreasing light intensity tend to inhibit a flowering.

A serious objection might be raised to the treatment of the nutrient problem in the Woods Hole area in that phosphate is the only factor considered in the equation. Lillick (1937) believed that nitrate was more important than phosphate in controlling phytoplankton production. This conclusion was based on two observations—first, that the seasonal trend of the nitrate curve was more closely correlated with phytoplankton than was the phosphate curve, and second, that the

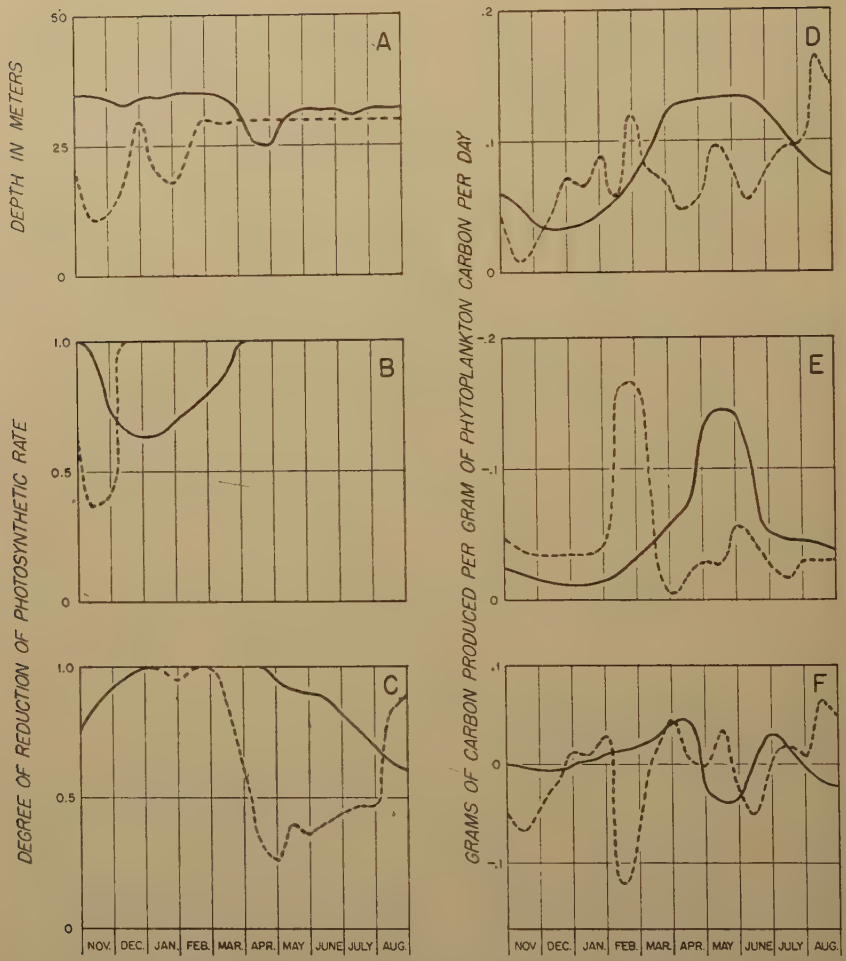

Figure 33. Comparison of environmental factors and phytoplankton growth processes on Georges Bank (solid line) and the Woods Hole area (broken line). A. The estimated depth of the euphotic zone (z_1) based on solar radiation and transparency. B. Reduction in photosynthetic rate by vertical turbulence ($1 - V$). C. Reduction in photosynthetic rate by nutrient depletion ($1 - N$). D. The calculated photosynthetic rate (P_h). E. The calculated grazing rate (G). F. The estimated rate of change of the population ($P_h - R - G$).

nitrate to phosphate ratio was lower than is the normal ratio found in the open oceans. If Lillick's argument is correct, the introduction of a nitrate factor will decrease the average rate of photosynthesis and will therefore change the form of the seasonal cycle. Unfortunately there is no very good quantitative information on the effect of nitrate on the photosynthetic rate. It appeared to be of little significance in the Georges Bank area; moreover, Ketchum (1939) found that 47 mgs. per m^3, the minimum concentration used in his experiments on *Nitzschia closterium*, did not reduce the growth rate. On the other hand Harvey (1933) found a difference in photosynthetic rate between cultures that were very deficient in nitrogen and others which had been enriched to the extent of 60 mgs. per m^3.

This fragmentary information does not lead to the formulation of a precise theory. Suppose, by way of experimentation, that the nutrient factor shall be the lower one of the following ratios: (a) the ratio of the phosphate concentration to 0.55 mg.-atom per m^3, or (b) the ratio of the nitrate concentration to a similar sort of maximum value for the limiting effect of nitrate. The largest value that can be postulated for this limiting effect is 47 mgs. of N per m^3. It will have the effect of reducing the average photosynthetic rate to 56 per cent of its previous value. The effect on the seasonal cycle of the phytoplankton population is shown in Fig. 34, in which the solid line is the crop as previously determined, and the broken line shows the effect of introducing a maximum nitrate factor. If the limiting nitrate concentration were reduced from 47 mgs., the effect on the photosynthetic rate would also be decreased, and at 20 mgs. there would no longer be a nitrate effect. It is evident, therefore, that depending on whatever assumption is made about nitrate limitation, the curves will fall somewhere between the limits drawn. It is also apparent that although the various assumptions alter the goodness of fit of the population curve, it is a skewing effect rather than a change in its essential features. There remains a rapid decrease from an autumn maximum, a late winter flowering, and no spring flowering of any consequence.

Although the original equation is a better fit for the data than the modification that includes a nitrate factor, it would be unfair on this basis alone to discount Lillick's theory of nitrate limitation. There remains the uncertainty of the evaluation of the grazing effect. Perhaps the assumptions on this subject over-rated the importance of small animals that escaped the scrim net. If this were true the estimate of the grazing rate should possibly be reduced to one-third or one-fifth the assigned value. This again skews the phytoplankton population curve and in extreme cases invalidates the comparison. A wide variety of results can be obtained by combining various assumptions

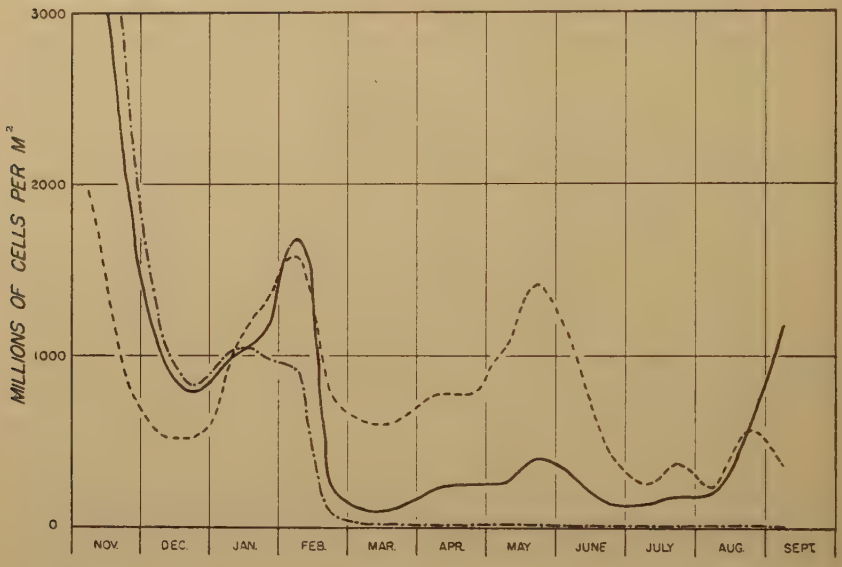

Figure 34. Comparison of different methods of calculating the theoretical population curves. Solid line, direct application of the Georges Bank equation. Broken line, introduction of a factor expressing the maximum possible effect of nitrate depletion. Dotted line, nitrate factor and reduction of grazing factor to one-third.

about the nitrate factor and the grazing effect. One is shown by a dotted line in Fig. 34, in which is assumed (a) maximum nitrate limitation, and (b) reduction of the grazing rate to one-third. It is a good fit for the data except that it postulates a secondary spring flowering in May which is almost as large as the February population. However, this may not be a very significant difference, since the calculation does not make allowance for grazing by the large spring crop of microcalanoids.

The results demonstrate the need for standard methods in regional surveys. Small differences in method may be of little importance in qualitative descriptions, but they assume major proportions as soon as quantitative comparisons are attempted. In the present case differences in methods of measuring the zooplankton in the two surveys are sufficient to prevent exact comparison. The assumptions that are made about this comparison of data determine to a large degree how accurately the Georges Bank equation fits the Woods Hole data. Nevertheless, changing the assumptions tends only to distort the curves rather than to destroy their distinguishing features. In no case does the curve resemble the Georges Bank seasonal cycle.

Therefore the results lend considerable credance to the view that differences in the seasonal cycles in the two areas are caused by rather small variations in the same basic group of six environmental factors. There is no evidence that the New England coastal populations must be explained by special phenomena such as species differences or the influence of land drainage.

SUMMARY

1. Previous studies of the phytoplankton in New England waters have shown that the seasonal cycle in coastal waters differs from that of the offshore banks in respect to the size of the spring flowering and its time of inception, the relative importance of summer and autumn flowerings, and the difference between maximum and minimum populations.

2. The reasons for these differences are investigated by comparing the seasonal cycles of Georges Bank and the coastal waters off Woods Hole. It had been found that the Georges Bank population was susceptible to a mathematical treatment such that seasonal variations in radiation, transparency, depth of the isothermal surface layer, the quantity of phosphate, temperature, and the amount of zooplankton could be combined in an equation which accurately predicted the phytoplankton cycle. The same equation is now applied to the Woods Hole data with a fair degree of success.

3. Certain difficulties are encountered in comparing the two populations because the methods used in the two surveys were not exactly the same. Assumptions must be made about how to convert the two sets of data into comparable terms, and this prevents precise application of the equation. Thus a variety of results is obtained, but in most of them a fair degree of success is obtained in fitting the equation to the data.

4. It is therefore probable that the differences between the observed populations in New England coastal waters and the offshore banks are the result of differences in simple environmental factors—transparency, stability, phosphate, etc.

APPENDIX

NUMERICAL VALUES USED TO CALCULATE THE RATE OF CHANGE OF THE WOODS HOLE PHYTOPLANKTON POPULATION. FOR EXPLANATION OF SYMBOLS SEE EQUATION (1) IN TEXT

Date		I_o	k	z_1	$1-V_1$	$1-N$	P_h	R	Z	gZ	P_h-R-G
Nov.	1	.132	.26	19	.63	1.00	.043	.048	6.3	.047	−.052
	15	.035	.33	11	.37	1.00	.009	.039	5.2	.039	−.069
Dec.	1	.094	.36	12	.40	1.00	.021	.032	4.7	.035	−.046
	15	.070	.24	18	1.00	1.00	.041	.027	4.7	.035	−.021
Jan.	1	.122	.14	30	1.00	1.00	.072	.024	4.7	.035	.013
	15	.125	.24	20	1.00	1.00	.065	.021	4.7	.035	.009
Feb.	1	.191	.30	17	1.00	.95	.087	.019	5.3	.040	.028
	15	.104	.18	25	1.00	1.00	.056	.018	21.4	.161	−.123
Mar.	1	.205	.14	30	1.00	1.00	.120	.018	22.2	.167	−.065
	15	.188	.18	29	1.00	.87	.078	.021	6.0	.045	.012
Apr.	1	.243	.18	30	1.00	.62	.069	.023	.4	.003	.043
	15	.205	.12	30	1.00	.33	.047	.023	2.3	.017	.007
May	1	.333	.13	30	1.00	.26	.055	.029	3.7	.028	−.002
	15	.382	.13	30	1.00	.40	.096	.036	3.6	.027	.033
June	1	.312	.13	30	1.00	.36	.082	.046	7.5	.056	−.020
	15	.229	.14	30	1.00	.40	.055	.058	6.4	.048	−.051
July	1	.354	.16	30	1.00	.44	.077	.049	3.6	.027	.001
	15	.320	.13	30	1.00	.47	.094	.061	2.0	.015	.018
Aug.	1	.350	.14	30	1.00	.47	.097	.060	4.0	.030	.007
	15	.343	.14	30	1.00	.82	.165	.068	4.0	.030	.067
Sept.	1	.274	.14	30	1.00	.89	.143	.064	4.0	.030	.049

REFERENCES

BIGELOW, H. B.

1926. Plankton of the offshore waters of the Gulf of Maine. Bull. U. S. Bur. Fish., *40:* 1–509.

BIGELOW, H. B., L. C. LILLICK AND MARY SEARS

1940. Phytoplankton and planktonic protozoa of the offshore waters of the Gulf of Maine. I—Numerical distribution. Trans. Amer. phil. Soc., (N S) *31* (3)*:* 149–191.

CLARKE, G. L.

1938. Seasonal changes in the intensity of submarine illumination off Woods Hole. Ecology, *19* (1)*:* 89–106.

CLARKE, G. L. AND D. F. BUMPUS

1940. The plankton sampler—an instrument for quantitative plankton investigations. Spec. Publ. Limnological Soc. Amer., No. *5:* 1–8.

CLARKE, G. L. AND D. J. ZINN

1937. Seasonal production of zooplankton off Woods Hole with special reference to *Calanus finmarchicus.* Biol. Bull. Wood's Hole, *73* (3)*:* 464–487.

Fleming, R. H.
1939. The control of diatom populations by grazing. J. Cons. Explor. Mer., *14* (2): 210–227.
Harvey, H. W.
1933. On the rate of diatom growth. J. Mar. biol. Ass. U. K., (N S) *19:* 253–276.
Ketchum, B. H.
1939. The absorption of phosphate and nitrate by illuminated cultures of *Nitzschia closterium.* Amer. J. Bot., *26:* 399–407.
Lillick, L. C.
1937. Seasonal studies of the phytoplankton off Woods Hole, Massachusetts. Biol. Bull. Wood's Hole, *73* (3): 488–503.
Redfield, A. C.
1941. The effect of the circulation of water on the distribution of the calanoid community of the Gulf of Maine. Biol. Bull. Wood's Hole, *80* (1): 86–110.
Riley, G. A.
1946. Factors controlling phytoplankton populations on Georges Bank. J. Mar. Res., *6* (1): 54–73.
1947. A theoretical analysis of the zooplankton population of Georges Bank. J. Mar. Res., *6* (2): 104–113.

A MOMENTUM INTEGRAL FOR SURFACE WAVES IN DEEP WATER

By

Victor P. Starr

University of Chicago

It has been demonstrated by the studies of Stokes (1847) and Levi-Civita (1925) that surface waves of finite height which are irrotational and periodic can exist in a liquid under the influence of gravity. Furthermore, it was pointed out by Stokes that such waves produce a transport of mass in the direction of propagation and hence possess a certain horizontal momentum relative to the undisturbed water at great depths. The present purpose of the writer is to show that there exists a simple relationship between the momentum and the kinetic energy in such wave motion. An equation of similar form was first derived by Levi-Civita (1924) using a different approach, but, so far as the writer is aware, no oceanographic applications of it have been made.[1] It is possible that the relationship may be of significance in the study of wave growth due to wind action.

The theory for waves of finite amplitude, developed by the writers mentioned above, indicates that the waves are symmetrical about the crests and troughs, not only at the surface but also at greater depths, although there is a rapid diminution of the amplitude downward. This circumstance implies that there is no variation of phase of the waves with depth. Also the theory indicates that the speed of propagation is constant, and that the waves travel without alteration of their form at the surface or below. The fluid motions are assumed to take place without any viscosity being present, and relative to a non-rotating coordinate system, so that the treatment does not include the effects of Coriolis forces. Since there are no motions or variations in the motions in the direction parallel to the crests of the waves, it suffices to consider a vertical section across the crests as shown schematically in Fig. 35. The problem may thus be considered as one in two-dimensional motion.

We shall suppose that the actual waves are propagated from left to right in the figure, but in order to treat the problem as one in steady-state motion we shall suppose that a constant translation from right

[1] A somewhat similar relationship was derived by Rayleigh (1914) for the case of *long* waves by approximate methods.

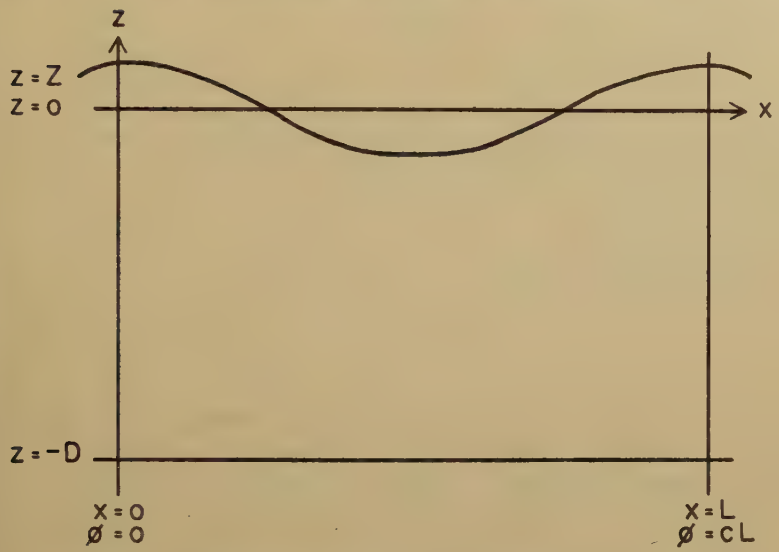

Figure 35. Schematic cross section of a wave normal to the wave crests.

to left, equal to the wave speed c, has been added to the actual motions. This artifice does not alter the fundamental properties of the dynamic system and produces greater simplicity in the picture of the motions. The vertical coordinate z is counted positive upward and has its origin in the undisturbed free surface of the water. The horizontal coordinate x is counted positive to the right and has its origin at a crest. The free surface Z is a streamline in the steady-state motion. Other streamlines similar to Z, but with progressively smaller amplitudes, lie below Z, but these are not shown in the diagram. The horizontal line $z = -D$ is assumed to be located at a sufficiently great depth where the wave disturbance is no longer of sensible intensity.

Since the motion is irrotational, it follows that we may introduce a velocity potential ϕ such that

$$U = -\frac{\partial \phi}{\partial x} \quad ; \; w = -\frac{\partial \phi}{\partial z}. \tag{1}$$

Here U is the particle velocity in the x-direction, and w is the particle velocity in the z-direction, in the steady-state motion. If drawn in the diagram, lines along which ϕ is constant would constitute a set of curves orthogonal to the streamlines, and hence it follows that ϕ has a constant value at the verticals $x = 0$ and $x = L$ (where L is the wave

length). The velocity potential is indeterminate to the extent of an arbitrary additive constant so that we may choose ϕ to be zero at $x = 0$. At the depth $z = -D$ the motion of the fluid is a simple horizontal translation at the rate c, so that here $U = -c$. Integration of the first equation in (1) thus gives the value for ϕ at $x = L$ to be cL.

By the use of Green's theorem it can be shown that the velocity potential obeys the following equation in a simply-connected space (see Lamb, 1932):

$$\int\int\int \left[\left(\frac{\partial\phi}{\partial x}\right)^2 + \left(\frac{\partial\phi}{\partial y}\right)^2 + \left(\frac{\partial\phi}{\partial z}\right)^2\right] dxdydz = -\int\int \phi \frac{\partial\phi}{\partial n} ds. \quad (2)$$

In this equation ds is an element of surface area of the volume considered, and $\partial\phi/\partial n$ is the derivative along the inward normal to this area. In our application of this relationship $\partial\phi/\partial y = 0$, and the volume integral becomes an area integral, since we are concerned with a section of unit thickness. The right-hand member of (2) becomes a line integral. Choosing the region bounded by the verticals $x = 0$ and $x = L$, the free surface Z and the line $z = -D$, the only nonvanishing contribution to the right-hand member of (2) results from the integration along the vertical at $x = L$, because $\phi = 0$ at $x = 0$ and $\partial\phi/\partial n = 0$ along the free surface and the line (streamline) $z = -D$. Since $\partial\phi/\partial n = +U_L$ at $x = L$, we get

$$\int_0^L \int_{-D}^{Z} (U^2 + w^2)\, dzdx = -cL \int_{-D}^{Z_L} U_L dz \quad (3)$$

after substitution from (1) in the left-hand member (Z_L is the value of Z at $x = L$). The integral on the right of (3) is simply the volume transport between the two streamlines considered, and hence we may replace it by a similar integral at an arbitrary vertical so that

$$\int_{-D}^{Z_L} U_L dz = \int_{-D}^{Z} U\, dz = \text{constant}. \quad (4)$$

Introducing the horizontal velocity component u, which is present in the actual wave motion, and which is related to U by the equation

$$U = u - c, \quad (5)$$

we may rewrite (3), after substituting from (4), as follows:

$$\int_0^L \int_{-D}^{Z} (u^2 + w^2 - 2cu + c^2)\, dzdx = -cL \int_{-D}^{Z} (u - c)\, dz. \qquad (6)$$

Since the area over which the integration extends is equal to LD because of the choice of the origin for z, it is possible to simplify (6) so that we have

$$\int_0^L \int_{-D}^{Z} (u^2 + w^2 - 2cu)\, dzdx + c^2LD = -cL \int_{-D}^{Z} u\, dz + c^2L\,(Z + D),$$

and finally,

$$\int_0^L \int_{-D}^{Z} (u^2 + w^2)\, dzdx - 2c \int_0^L \int_{-D}^{Z} u\, dzdx = -cL \int_{-D}^{Z} u\, dz + c^2LZ = K, \qquad (7)$$

where K is a quantity which is independent of x. From the last equality in (7) we obtain by integration over one wave length

$$K = -c \int_0^L \int_{-D}^{Z} u\, dzdx. \qquad (8)$$

If K is eliminated from (7) by means of (8) and the resulting equation multiplied by $\rho/2$, where ρ is the (uniform) density of the fluid, we obtain the relationship,

$$\int_0^L \int_{-\infty}^{Z} \rho \frac{u^2 + w^2}{2}\, dzdx = \frac{c}{2} \int_0^L \int_{-\infty}^{Z} \rho u\, dzdx. \qquad (9)$$

In view of the fact that the disturbance in the actual wave disappears at great depths, it is permissible to extend the integration downward to $-\infty$.

This last equation states that *the kinetic energy per wave length and per unit distance along the crests of the waves is equal to one half the wave speed multiplied by the momentum of the same water mass in the direction of wave propagation.* Once the distribution of the velocity potential in Fig. 35 has been specified, equation (2) can be applied in the manner described, not only to the region between the surface and depth D, but to any region bounded above and below by two streamlines and

by the two verticals at $x = 0$ and $x = L$. We might thus choose two streamlines, Z_1 and Z_2, which give a region whose area in the figure is numerically equal to L, and thus a volume in the section of unit thickness equal to L. For such a *material layer* we may then write

$$\frac{1}{L}\int_0^L\int_{Z_1}^{Z_2}\rho\frac{u^2+w^2}{2}\,dzdx = \frac{c}{2L}\int_0^L\int_{Z_1}^{Z_2}\rho u\,dzdx\,. \tag{10}$$

For the material layer considered, equation (10) states that on the average the kinetic energy per unit volume is equal to the momentum per unit volume multiplied by one half of the speed of propagation.[2]

It is of some interest to compare the value of the momentum given by equation (9) with the value obtained by Lamb (1932), who used the second order approximation to the wave solution presented by Stokes (1847). For this purpose it is necessary to have available an expression for the kinetic energy. Let us take for this quantity the approximate value given by the small-amplitude theory, namely, $\frac{1}{4}g\rho a^2L$, where a is the amplitude and g is the acceleration of gravity. Eliminating the product gL from this expression by means of the relation that $2\pi c^2 = gL$, also given by the small-amplitude theory, and placing the result into (9), we obtain the expression $\pi\rho a^2c$ for the momentum per wave length. This is in agreement with the result obtained by Lamb, except that in Lamb's result a is, strictly speaking, not the amplitude but rather an amplitude parameter which becomes very nearly equal to the amplitude for waves of small height. It should be remarked, however, that both the present method and the method used by Lamb for obtaining the momentum are approximate [although relation (9) is an exact one].

The extent to which the theoretical results obtained in this paper are directly applicable to surface waves which actually occur in the ocean is, of course, an open question. The waves which are found in nature are irregular in general, and the medium in which they are found departs considerably in its properties from an ideal fluid. Moreover, the motions take place in a rotating coordinate system so that it would appear that Coriolis forces are of importance in connection with the momentum associated with the waves, although such forces are probably of negligible consequence as far as the purely oscillatory components of motion are concerned. Temporarily laying

[2] This relationship is analogous to the principle in the electromagnetic theory of light, which states that in the case of plane waves the energy per unit volume is equal to the electromagnetic momentum per unit volume multiplied by the speed of propagation (see Page and Adams, 1931).

aside all such difficulties, it is a matter of at least some academic interest to see what use might be made of equation (9) in the study of the growth of waves due to wind action. The possible utility of the equation for this problem lies in the fact that, whereas it is a matter of great difficulty to estimate the energy imparted to the sea surface by a given wind, estimates of the momentum transfer are more easily made.

For this purpose let us substitute the approximate values mentioned above for the energy per wave length and for the wave speed c, given by the small-amplitude theory, into (9). The result may then be written in the form

$$g\rho a^2 = 2\sqrt{\frac{gL}{2\pi}}M, \tag{11}$$

where M is the average wave momentum per unit area of the sea surface. We shall assume that the wave system considered remains under the influence of a uniform wind which feeds energy and momentum into it during a given period of time. Since for a given wave length there is a limit to the amount of energy which can thus be fed into the waves, beyond which the waves break, it must be assumed that such breaking does take place and that longer waves with greater momentum and energy capacities are continually generated. For this reason it might be expected that the ratio of the amplitude a to the wave length L should be relatively large. The theoretical limiting value for this ratio is about 1/14, but it would be unreasonable to expect that this value would be reached due to the observed irregularities in the waves and to the presence of waves which have not attained the maximum height. As a more reasonable supposition, let us take an average value of 1/24, so that we have

$$\frac{a}{L} = \frac{1}{b} = \frac{1}{24}. \tag{12}$$

Eliminating the amplitude a from (11) by means of (12) and solving for L, we obtain

$$L = \sqrt[3]{\frac{2b^4M^2}{\pi g\rho^2}}. \tag{13}$$

Assuming, for purposes of orientation, that the total momentum transferred from a steady wind over a period of time t is used in creating waves on an originally undisturbed sea, we have

$$M = \tau t. \tag{14}$$

Here τ is the tangential wind stress and hence is the rate at which momentum is imparted to the sea. Rossby (1936) has given a relationship for obtaining the stress τ in terms of the wind velocity, namely

$$\tau = \rho^* \gamma_h^2 W_h^2 , \tag{15}$$

ρ^* being air density, W_h the wind at height h and γ_h a resistance coefficient appropriate for the level h. If h is approximately 15 meters, the value of γ_h is about 5×10^{-2} when c.g.s. units are used. According to this formula a wind of 30 knots should produce a stress of about 7 dynes per square centimeter.[3]

With such a stress equations (13) and (14) give the result that waves about 430 meters in length should be generated in 24 hours. The period of such waves would be about 16.6 seconds.[4] Since waves of this magnitude are seldom if ever observed in the generating areas, even with stronger winds than we have assumed, it seems that some of the premises made above are not proper.

The effect of the tangential wind stress on the motions of water in the oceans was treated by Ekman (1905), and the results of his studies are well known to oceanographers. In the present discussion the question arises whether the mass transport associated with wave motion is in some manner an integral part of the drift currents in the theory of Ekman, or whether it is superimposed on the drift currents. As a third possibility, it may perhaps be that, since the wave transport is not dependent on the presence of internal viscosity, but is, on the

[3] Formula (15) is applicable when the sea surface is hydrodynamically "rough." This condition is present with wind velocities above about 10 knots. The derivation of this equation indicates that τ is the total rate of momentum transfer to the sea surface regardless of the details of the mechanism by means of which this transfer is effected in the immediate vicinity of the water surface.

[4] According to the small-amplitude theory, there exists an equation relating the wave period T to the wave length L. The wave length may be eliminated from this equation by means of (13). We thus have $T = \sqrt{\frac{2\pi L}{g}}$, which becomes $T = \sqrt[3]{\frac{4\pi b^2 M}{g^2 \rho}}$. If τ and b are constant, it follows, with the aid of (14), that *the period T is proportional to the cube root of the time.* Under these circumstances we may also obtain by differentiation that

$$\frac{1}{T}\frac{dT}{dt} = \frac{1}{3t}, \text{ and } \frac{1}{L}\frac{dL}{dt} = \frac{2}{3t},$$

showing that the percentage rate of increase of the period or wave length is inversely proportional to the time. Similar equations may be written for the wave speed c.

other hand, subject to the effects of Coriolis forces, a composite solution to the problem can exist which takes into account these properties of the wave-transport components of the total motion. Whatever the answer to this question may be, it seems reasonable to suppose that not all of the momentum which is imparted to the sea by the wind stress goes into wave momentum, but that most of it is utilized in the generation and maintenance of drift currents. It is thus not surprising that the calculation of the magnitude of waves generated by a given wind on the assumption that all the momentum transferred becomes wave momentum should give too intense wave action. In order to use equation (13) for the purpose of securing an estimate of the waves which are actually generated, it would thus be necessary to have available a criterion to determine what fraction of the momentum goes into the wave motion.

Carrying these speculations a step further, it may be that during the growth of wave motion the fraction of the momentum which is used in creating waves changes as time progresses. Since the development of drift currents is dependent upon the presence of eddy viscosity in the water, and since this turbulent viscosity is relatively small during the early stages of the process, it is not unreasonable to suppose that at the beginning a relatively large part of the momentum received is utilized in a rapid development of wave motion. On the other hand, during the later stages of the process the continued presence of breaking waves probably brings about a large increase in the turbulent viscosity which in turn renders possible the existence of well developed drift currents whose maintenance requires a large part of the momentum received, so that but little remains for a further increase in the wave action. In the end some sort of steady state would thus be indicated, in which practically all of the momentum goes into the maintenance of drift currents and no further growth of the waves takes place, unless the wind conditions should change. That some such steady state does finally develop with a constant wind is supported by the fact that there is normally no progressive change in the wave regime in the large oceanic regions in the trade-wind belts.

The writer wishes to express his gratitude to Dr. C.-G. Rossby for many fruitful discussions of the matters touched upon in this paper, and to Dr. J. Charney and Mr. D. Fultz for reading the manuscript.

[*Note*—As this paper is going to press the writer has had opportunity to read a very interesting article by Sverdrup and Munk (1946) dealing with the subject of wave generation through wind action. These authors present curves depicting the increase of wave height and wave speed with time for an unlimited fetch under the influence of a constant wind (fig. 3 in their paper). These curves are derived on

the basis of energy transfer calculations and have been used in the forecasting of wave formation for practical purposes.

If we accept these results obtained by Sverdrup and Munk as representing the actual process of wave generation, casual inspection of the curves shows that in the earlier stages the wave height increases as the two-thirds power of the time and the wave speed increases as the one-third power of time. This is in agreement with the equations contained in the present paper, provided that the parameter b is constant. Numerical computation shows, moreover, that with $b = 24$ (steepness about eight per cent), *approximately ten per cent of the momentum received by the water becomes wave momentum during these early stages.* During the later stages both curves tend to level off showing that probably a smaller and smaller percentage of the momentum received is utilized in wave growth.]

SUMMARY

In this paper an integral relationship between the kinetic energy and horizontal momentum of surface waves is derived by simple methods. A relation of similar form was first derived by T. Levi-Civita who used a different approach. The equation obtained by the writer states that the kinetic energy per wave length and per unit distance along the crests of the waves is equal to one half the wave speed multiplied by the momentum of the same water mass in the direction of wave propagation.

An attempt is made to utilize this equation for the study of the growth of waves due to wind action. The possible utility of the equation in this problem lies in the fact that, whereas it is difficult to estimate the energy imparted to the sea surface by a given wind, estimates of the momentum transfer are more easily made. For the case of an initially undisturbed ocean of large dimensions, subjected to a constant and uniform wind, a formula is obtained which states that the wave length should increase as the two-thirds power of the time. Numerical computations show that the wave lengths thus obtained are too large. It is suggested that the discrepancy may be due to the fact that a certain fraction of the momentum absorbed by the water is utilized in the generation and maintenance of drift currents. Further study may show that it is possible to introduce corrections for such effects.

REFERENCES

Ekman, V. W.
1905. On the influence of the earth's rotation on ocean-currents. Ark. Mat. Astr. Fys., *2* (11): 1–52.

Lamb, Horace
1932. Hydrodynamics. Cambridge Univ. Press, sixth ed. pp. 43–47 and 417–420.

Levi-Civita, Tullio
1924. Questioni di meccanica classica e relativista, II. Zanichelli, Bologna. pp. 26–59. (German translation, Julius Springer, Berlin.)
1925. Détermination rigoureuse des ondes permanentes d'ampleur finie. Math. Ann., *93:* 264–314.

Page, Leigh and N. I. Adams
1931. Principles of electricity. Van Nostrand Co., New York. pp. 575–579.

Rayleigh, Lord
1914. Further calculations concerning the momentum of progressive waves. Phil. Mag., (6) *27:* 436–440.

Rossby, C.-G.
1936. On the momentum transfer at the sea surface. I. On the frictional force between air and water and on the occurrence of a laminar boundary layer next to the surface of the sea. Pap. phys. Oceanogr., *4* (3): 3–20.

Stokes, G. G.
1847. On the theory of oscillatory waves. Trans. Camb. phil. Soc., *8:* 441–455. (Also in Stokes' *Mathematical and physical papers, 1*, 1880: 197–229, 314. Cambridge Univ. Press)

Sverdrup, H. U. and W. H. Munk
1946. Empirical and theoretical relations between wind, sea, and swell. Trans. Amer. geophys. Un., *27* (6): 823–827.

NOTE ON THE CORRECTION OF REVERSING THERMOMETERS[1]

By

H. U. SVERDRUP

Scripps Institution of Oceanography, University of California
La Jolla, California

Corrections have to be applied to the readings of protected and unprotected reversing thermometers because they are read at a temperature that differs from that at the time of reversal. In deriving these corrections it is generally assumed that Feruglio's (1912) equation [(5) below] is exact. It is shown here that Feruglio's equation is not quite exact, but a close approximation. From this equation practical formulae, equations (6) and (8) below, can be derived very simply without further sacrifice of accuracy.

PROTECTED THERMOMETERS

Notations.

T_w	: true water temperature at reversal.
T	: reading of reversing thermometer.
I	: index correction of thermometer.
$T' = T + I$	: reading of reversing thermometer corrected for index error.
$\Delta T = T_w - T'$	: correction to be applied with proper sign to reading in order to obtain true water temperature ($T_w = T' + \Delta T$).
v_o	: volume of mercury below scale division "0 degree," expressed in °C.
$v_w = v_o + T_w$	: volume of mercury at true water temperature.
$v_t = v_o + T'$	: volume of mercury at reading.
t	: temperature of auxiliary thermometer, that is, temperature of main thermometer at reading.
$1/K$	: coefficient of thermal expansion of system glass-mercury expressed in unites $°C^{-1}$. For Jena glass 59^{III}, $K = 6100$, and for Jena glass 16^{III}, $K = 6300$.

[1] Contribution from the Scripps Institution of Oceanography, New Series, No. 304. This work represents results of research carried out for the Hydrographic Office, the Office of Naval Research, and the Bureau of Ships of the Navy Department under contract with the University of California.

The change in volume of the torn-off column of mercury is

$$dv = \frac{1}{K} v dt . \tag{1}$$

Therefore, assuming K to be constant in the temperature range T_w to t:

$$\int_{T_w}^{t} \frac{dv}{v} = \frac{1}{K} \int_{T_w}^{t} dt , \tag{2}$$

or

$$ln \frac{v_t}{v_w} = \frac{1}{K} (t - T_w) = - (T_w - t) \frac{1}{K} . \tag{3}$$

Since

$$v_t = v_0 + T' = v_0 + T_w - \Delta T ,$$

$$v_w = v_0 + T_w ,$$

it follows

$$ln \frac{v_t}{v_w} = ln \left(1 - \frac{\Delta T}{v_0 + T_w} \right) = - \frac{T_w - t}{K} . \tag{4}$$

Expanding the logarithm in series and omitting terms, which, if retained, would result in a maximum error in ΔT of 0.002°, one obtains Feruglio's (1912) formula:

$$\Delta T = \frac{(T_w - t (v_0 + T_w)}{K} . \tag{5}$$

Introducing $T_w = T' + \Delta T$ and omitting a term containing $(\Delta T)^2$:

$$\Delta T = \frac{(T' - t) (v_0 + T')}{K - (T' - t) - (v_0 + T')} . \tag{6}$$

This formula is nearly identical with the formulae by Schumacher (1923) and Hidaka (1932), but it is slightly more accurate. The advantage of the present derivation is that formula (4) is exact if K is a constant and that any desired degree of accuracy can be achieved by taking more terms into account when expanding the logarithm in (4) in series. This is in effect done by Hansen (1934).

In the above, the index correction has been applied before computing ΔT, but in practice this refinement is not necessary if the index correction is less than 0.1°. In (6) T' can be replaced by T, the reading of the reversing thermometer, and the index correction can be combined with ΔT to give the total correction. Furthermore, since the numerical value of the sum $(T' - t) + (v_0 + T')$ generally is about 100, the

denominator in (6) can be taken as 6000 or 6200 for Jena glass 59^{III} and 16^{III} respectively.

UNPROTECTED THERMOMETERS

Notations. As above, adding subscript u to reading and corrected values of unprotected thermometer. Thus $T_{w,u}$ represents the true value recorded by the unprotected thermometer at reversal and $\Delta T_u = T_{w,u} - T_u'$.

Equations (1) to (3) remain unaltered but (4) becomes

$$ln \frac{v_t}{v_w} = ln \left(1 - \frac{\Delta T_u}{v_o + T_{w,u}}\right) = - \frac{T_w - t}{K}, \tag{7}$$

which is exact if K is constant. Expanding the logarithm and introducing $T_{w,u} = T_u' + \Delta T_u$ leads to the close approximation:

$$\Delta T_u = \frac{(T_w - t)\,(v_o + T_u')}{K - (T_w - t)}. \tag{8}$$

Equation (8) is nearly identical with Schumacher's formula (1923).

REFERENCES

FERUGLIO, G.
1912. Il termometro a rovesciamento . . . R. Com. Tallassogr. Ital., Memoria VII, Venedig.

HANSEN, WALTER
1934. Bemerkungen zu den Korrektionsformeln für das Tiefsee-Umkippthermometer. Annalen Hydrogr., Berl., Jg. 62: 145–147.

HIDAKA, KOJI
1932. Ueber eine neue Korrektionsformel zur Umkippthermometerablesung. Mem. Mar. Obs. Kobe, *5:* 10–13.

SCHUMACHER, ARNOLD
1923. Neue Hilfstafeln für die Umkippthermometer nach Richter und Beiträge zur thermometrischen Tiefenmessung. Annalen Hydrogr., Berl., Jg. 51: 273–280.

A SALINOMETER FOR USE IN BRACKISH WATER[1]

By

WILLIAM S. VON ARX

Woods Hole Oceanographic Institution

In principal this salinometer is a "battery" composed of a pair of dissimilar metals immersed in the brackish water of the field as an electrolyte. Between these dissimilar metals there exists a potential difference which is practically independent of the concentration of salts in the electrolyte over a very wide range. However, the salt concentration has a marked effect upon the conductivity of the electrolyte. If the measuring circuit has constant resistance, the only change of resistance in the total circuit is that due to the change of conductivity of the water in which the cell is immersed. Since the driving EMF is essentially constant, the current flowing in the circuit is a measure of the conductivity of the water sample.

The conductivity of salt solutions varies with both salt concentration and temperature, an increase of either quantity in dilute solution producing an increase in conductivity. Fortunately there is a way to neutralize the changes of conductivity due to changes of temperature, leaving only those due to changes of salinity. Aqueous salt solutions have a negative temperature coefficient of resistance while most metals have a positive one. It is a simple matter, therefore, to place in series with the cell and in thermal contact with the water a wire resistor having a positive thermal coefficient and a numerical change of resistance both equal and opposite to that of the water sample. This method of temperature compensation is not exact for all salinities, since the temperature coefficient of resistance of salt solutions changes with the salt concentration, but the errors are small. A midrange salinity can be chosen in accordance with the demands of the field problem and the change of resistance (ΔR) of the cell measured over the range 0 °C., to 30 °C.; (ΔT). Knowing α, the temperature coefficient of resistance for the metal wire compensator, one can calculate the room temperature resistance (R_o) needed to compensate the cell.

$$R_o = \frac{(\Delta R)}{\alpha\,(\Delta T)}$$

[1] Contribution No. 370 from the Woods Hole Oceanographic Institution.

Figure 36. (*Left*)—Side view showing part of 50 feet of cable, underwater unit, and the stowage compartment for both. The temperature compensating resistor winding is on top of the disc-shaped underwater unit. The complete instrument weighs 22 pounds and occupies less than one cubic foot of space. (*Right*)—Front view showing the salinity indicator (white dial), the polarization current indicator (black dial), with the calibration knob between. In the lower bank (left to right) are polarization current limiter, battery switch, salinity indicator switch, reading switch, and the range selector. Note the calibration chart in the lid, as well as the ring electrodes and perforations in the underwater unit.

Nickel wire 0.010 inches in diameter, having an $\alpha = 0.006$ ohms/°C., has been found most suitable. The cell itself can be built of practically any combination of metals or substances susceptible to strong and lasting polarization, such as Carbon. Experiments with many combinations show Copper and Zinc to be electrically and chemically suitable. The physical shape of the Cu-Zn pair is relatively unimportant and may be altered to suit the requirements of the investigation. A problem presented to the writer was the measurement of the salinity of thin layers of terrigenous fresh water floating on, and mixing with, sea water in a small estuary which was being used for ecological studies (Edmondson, 1947). The electrode shape finally chosen was a pair of concentric horizontal rings a few millimeters in height. These, together with a flat ring of lucite on which the compensating resistance wire was wound, produced a cylindrical underwater unit

1 cm. high and 10 cm. in diameter which was so thoroughly pierced with large holes that it disturbed the water only slightly when lowered through the boundary between stratified water layers. Through efforts to maintain lowest possible cell resistance, it was found that twice as much Zinc surface as Copper surface was needed. For this reason the outer ring was made of Zinc and the inner one of Copper.

This ratio of areas is also found to be best in the case of flat plates. Long narrow plates are more efficient than square ones. Efficiency is gauged in terms of the largest current passed through the measuring circuit when comparing electrodes of the same area and spacing but different shape. Long narrow electrodes also have the least "surface error": specifically, a reduction of current in the measuring circuit due to the electrodes being quite near the liquid surface boundary across which the ion field cannot develop. Electrodes having an aspect ratio greater than 10 to 1 can be brought within 0.5 of a ratio unit of the surface before surface effects become serious. This is less than the practical limit, since the temperature compensator is then out of water.

The preparation and use of Copper-Zinc electrode pairs involves a simple preliminary technique. A new Copper-Zinc electrode pair immersed in a saline solution develops an EMF instantly, but the current flowing between the plates is subject to rapid change, ultimately subsiding to a vanishing quantity. This is due to the insulating effects of the reaction products on the plates through which most of the initial potential drop is eventually consumed. To avoid this effect an outside EMF, larger than that of the cell, is applied to drive the cell backward producing a copious emission of bubbles (H_2) at the Zinc plate. Thirty seconds of treatment at one ampere prepares the electrodes for use. During the counter polarization treatment a number of compounds are developed on both electrodes (Bengough and May, 1924). The Zinc electrode is oxidized and eventually develops a white coating of $ZnCO_3$ upon exposure to air. The Copper electrode at first becomes yellow with $CuCl_2$, Cu_2O and, in the presence of sufficient oxygen, $Cu_4(OH)_6Cl_2 \cdot H_2O$, turning yellow-green and finally blue-green upon exposure to air. The final coating is mossy or slightly botryoidal, its color being determined by the preponderance of Malachite $CuCO_3 \cdot Cu(OH)_2$ [the basic Cupric Carbonate developed in the presence of atmospheric CO_2], and Cupric Oxychloride $CuCl_2 \cdot 2\,CuO \cdot 4\,H_2O$.

After preparation the behavior of the electrodes is quite changed, as is shown in Fig. 37. Upon immersion in the water sample the current at first falls off rapidly, then more slowly, and finally, in a matter of 10 seconds all told, it assumes a constant value which is maintained for several minutes before beginning the asymptotic decline toward

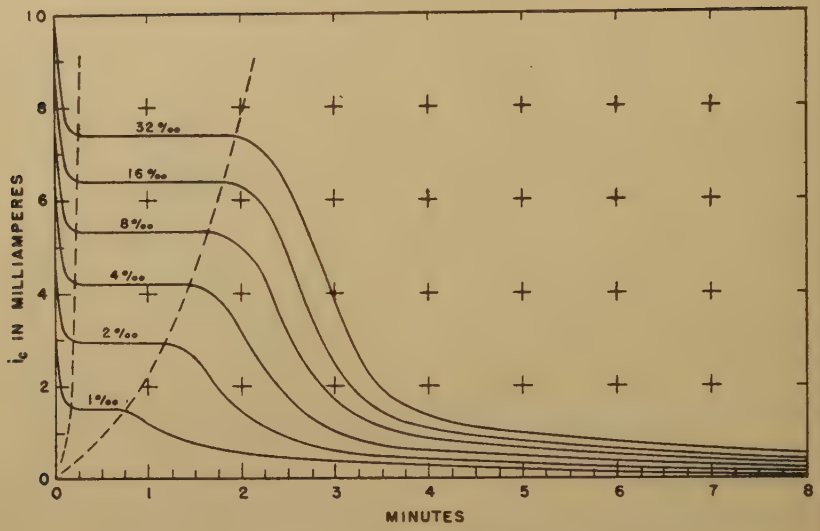

Figure 37. Current Variation with Time at Different Salinities,

zero. The plateau value is the one which is useful in salinity measurement. It is thought that this plateau is produced by the slow solution of the chemical products of counter-polarization. The plateau lasts longer in high salinity water than in low, suggesting that the rate of solution is controlled by the concentration of salts around the electrodes. Counterpolarization is complete when the current output of the electrodes, immediately after recharging, has a plateau in its time rate of decline. The plateau results from a certain number of coulombs of charge having been passed backwards through the cell. The length of the plateau in time is not conspicuously increased by an overdose of charge but the time required for the plateau to be reached is measurably increased. For this reason it is helpful to place an ammeter in series with the counterpolarizing EMF. Its reading is at first 10 per cent higher than later, a sudden drop indicating when the counterpolarization process is complete.

The salinometer circuit, including that of the underwater unit, is given in Fig. 38. The principal control is the "reading switch," a double-throw, single-pole switch that automatically cuts out the salinity-indicating milliammeter whenever the counterpolarizing current is cut in. Calibration is accomplished by means of a variable resistor in series with the salinity indicator. A bottled sample of water of known salinity must be carried along for calibration purposes. After the underwater unit has been counterpolarized for a minute or so to

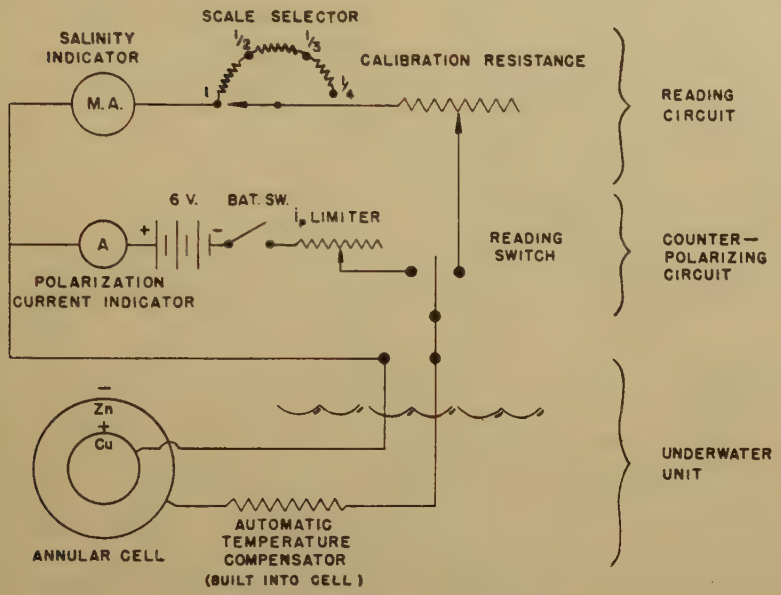

Figure 38. Salinometer Circuit Diagram.

insure the restoration of the deposits on the electrode surfaces and their thorough saturation with water, the reading switch is thrown and the system is allowed to come to equilibrium in the calibration sample. By adjustment of the resistance of the reading circuit the milliammeter can be made to read properly the salinity of the known sample based upon the original calibration curve made in the laboratory from a series of other known samples. In the field, calibration at only one point is sufficient to bring the whole scale of values into proper alignment. Recalibration is desirable every now and then to be sure that mechanical shifting caused by inadvertent bumping of the instrument, or the sun's heat, has not changed the preliminary calibration.

The calibration curve for the instrument is exponential in appearance, but it follows no true exponential function as far as is known. A family of such curves for different temperatures is shown in Fig. 39. These curves were determined by cutting a sample of sea water of prearranged temperature and known salinity with fresh water at the same temperature, counterpolarization having been standardized at 15 seconds and applied before each reading. The cuts were made in the ratios 1/1, 1/2, 1/4, 1/8, 1/16, 1/32, these being successive cuts each by

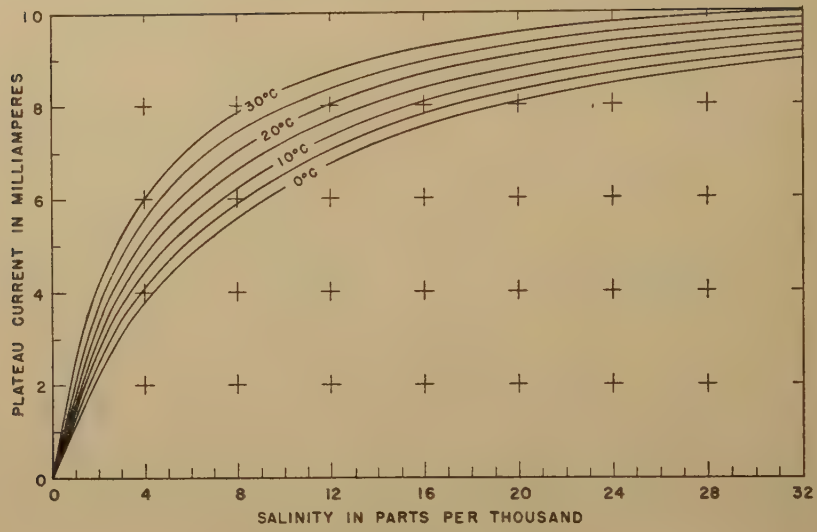

Figure 39. Characteristic Calibration Curves for Various Temperatures.

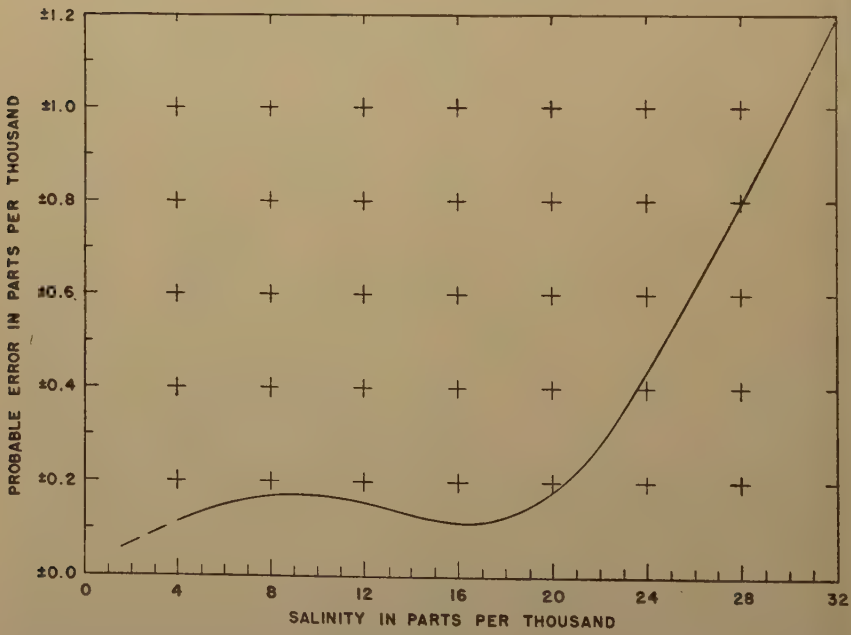

Figure 40. Residual Errors Including Reading Error After Temperature Compensation at 20° C. and 16°/oo.

half of an original volume. With a temperature compensated cell only one or two such runs need be made, and these without excessive attention to temperature. It will be noted that the shape of the calibration curve is such that the accuracy of measurement increases as the salinity diminishes. In addition to this scale convergence there is a milliammeter reading error of approxiamtely ± 2 per cent of the full scale deflection which arises in part from the error of the eye in reading the meter and in part from errors in the reproducibility of the pointer movement itself. These errors, together with those remaining after temperature compensation, are given in Fig. 40, which assumes the temperature error to be zero at 20° C.

Of the salinometers in use at present, this salinometer is less accurate and more sensitive to temperature than others. But it has the great advantage of portability, which, together with its simplicity, wide range and ease of calibration, makes it useful for programs of work where the salinity gradients are large and abrupt, or where it is desirable to measure the initial thickness and mixing zones of excessively thin layers of water. It is also inexpensive to build and maintain.

Mr. T. Wehe has earned the writer's gratitude for his painstaking assistance in making repeated thermal calibration runs and experiments with a large variety of electrode sizes and compositions.

SUMMARY

The salinometer is a simple electrical instrument for direct measurements in the field of a wide range of salinities. It is particularly well suited for use from a skiff, since it is light, portable and readily calibrated in the field. Because the approach is simpler, the instrument is described in terms of empirical relationships between the experimental variables rather than rigorously in terms of physical chemistry. From the experimentally derived curves the behavior of the instrument can be predicted sufficiently well for purposes of design and readaptation to special investigations.

REFERENCES

Bengough, G. D. and R. May
1924. Seventh report to the Corrosion Research Committee of the Institute of Metals. J. Inst. Met., *32:* 81 ff.

Edmondson, W. T.
1947. (In MS.)

NOTE TO AUTHORS

The pages of this Journal are open to all contributors, and manuscripts may be submitted to any member of the Board of Editors or to the Managing Editor. Publication will be made only in the English language, but copy may be submitted for consideration in other languages. Aid in translation of accepted manuscripts will be given when possible.

All manuscripts should be typewritten with double space, carefully corrected, with footnotes continuously numbered and set off in the body of the text. If an article is to appear as a contribution from another institution, it should be approved by that institution before submission; contribution numbers of such institutions are submitted with the return of galley proofs.

Each author receives 50 reprints (with covers) free of charge up to a maximum of 150 free reprints of any single article in the case of joint authorship by three or more authors. Additional reprints with or without covers may be ordered by authors or institutions at the cost of printing. Orders for reprints are given when galley proofs are returned.

Both galley and page proofs are submitted to the senior author of each article.

Tables should be prepared for clarity and as near as practicable to Journal pattern, without ruled lines if possible. Table footnotes should appear at the base of each Table.

Figures are required for consideration simultaneously with the manuscript. Original figures of inconvenient size for forwarding may be represented by photographs on first submission of a manuscript; originals are required for line cuts. Illustrations requiring half-tone reproduction should be avoided as far as possible, but they will be accepted when necessary. *It is very important that the proper size of characters and symbols should be used for the lettering of illustrations.* A diagram for determining suitable heights of letters for original drawings that will be reduced, together with an explanatory note, has been published in this Journal, Vol. III, No. 1: 89–91; reprints will be submitted to authors on request. Mechanical lettering is recommended. If facilities for lettering are not available to the author, it is preferable to receive illustrations with lettering indicated in pencil only, to be finished in ink in the editorial office. All illustrations will be subject to at least a minimum reduction at the rate of 1 : 1.2. Drawings which have been heavily patched and pasted must *not be rolled* for mailing. The legends for the figures, identified by corresponding figure numbers on the illustrations also, should be typed in sequence at the end of the manuscript.

A complete and *accurate list of references* in alphabetical order at the end of each article is essential. References may be indicated in the text by author's name (or names) and *year of publication*, or by italicized numbers which correspond to the numbers given in sequence in the list of references. Each reference should include the last name followed by at least two initials or first name; co-authors should be listed with the initials or first name preceding the last name. The date should be indented on the line below, followed by a complete title *verbatim* in lower case except for the first word. Publisher, city and pagination should be indicated for books; for periodicals (abbreviations from "World List of Scientific Periodicals," Oxford, as far as possible), the volume (italicized), number and pagination should be given.

Additional information regarding the preparation of manuscripts will be furnished by the Managing Editor.

TABLE OF CONTENTS

	Page
1. **Henry Stommel:** Note on the use of the *T-S* correlation for dynamic height anomaly computations	85
2. **C.-G. Rossby:** Notes on the distribution of energy and frequency in surface waves	93
3. **G. A. Riley:** A theoretical analysis of the zooplankton population of Georges Bank	104
4. **G. A. Riley:** Seasonal fluctuations of the phytoplankton population in New England coastal waters	114
5. **V. P. Starr:** A momentum integral for surface waves in deep water	126
6. **H. U. Sverdrup:** Note on the correction of reversing thermometers.	136
7. **W. S. von Arx:** A salinometer for use in brackish water	139

REQUEST FOR PUBLICATIONS

At the present time there is an urgent need for American publications to restock the libraries of the world, especially in the devastated areas. The American Book Center for War Devastated Libraries, Inc., Library of Congress, Washington 25, D. C., has been created to meet this need, and its primary function is to collect and ship abroad scholarly books and periodicals which will be necessary in research and in the physical, economic, social and industrial rehabilitation and reconstruction of Europe and the Far East. The Center cannot purchase books and periodicals; it depends on gifts from individuals and institutions. Because of limited shipping facilities, materials must be carefully selected, and therefore emphasis is placed upon publications issued during the past decade, upon scholarly books, periodicals, fiction and non-fiction of distinction in all fields, but especially in the sciences and technologies. All shipments should be sent prepaid to the above Center.